Review
Science with Neutrino Telescopes in Spain

Juan José Hernández-Rey [1,*], Miguel Ardid [2], Manuel Bou Cabo [3], David Calvo [1], Antonio F. Díaz [4], Sara Rebecca Gozzini [1], Juan A. Martínez-Mora [2], Sergio Navas [5], Diego Real [1], Francisco Salesa Greus [1,*], Agustín Sánchez Losa [1], Juan de Dios Zornoza [1] and Juan Zúñiga [1]

1   IFIC—Instituto de Física Corpuscular, Universitat de València and CSIC, C/Catedrático José Beltrán, 2, 46980 Paterna, Spain; dacaldia@ific.uv.es (D.C.); sara.gozzini@ific.uv.es (S.R.G.); real@ific.uv.es (D.R.); agustin.sanchez@ific.uv.es (A.S.L.); zornoza@ific.uv.es (J.d.D.Z.); juan.zuniga@ific.uv.es (J.Z.)
2   Instituto de Investigación para la Gestión Integrada de las Zonas Costeras, Universitat Politècnica de València, C/ Paranimf, 1, 46730 Gandia, Spain; mardid@fis.upv.es (M.A.); jmmora@fis.upv.es (J.A.M.-M.)
3   Instituto Español de Oceanografía, Unidad Mixta IEO-UPV, C/Paranimf, 1, 46730 Gandia, Spain; manuel.bou@ieo.es
4   Department of Computer Architecture and Technology/CITIC, University of Granada, 18071 Granada, Spain; afdiaz@ugr.es
5   Departamento de Física Teórica y del Cosmos and C.A.F.P.E., University of Granada, 18071 Granada, Spain; navas@ugr.es
*   Correspondence: juan.j.hernandez@ific.uv.es (J.J.H.-R.); sagreus@ific.uv.es (F.S.G.)

Abstract: The primary scientific goal of neutrino telescopes is the detection and study of cosmic neutrino signals. However, the range of physics topics that these instruments can tackle is exceedingly wide and diverse. Neutrinos coming from outside the Earth, in association with other messengers, can contribute to clarify the question of the mechanisms that power the astrophysical accelerators which are known to exist from the observation of high-energy cosmic and gamma rays. Cosmic neutrinos can also be used to bring relevant information about the nature of dark matter, to study the intrinsic properties of neutrinos and to look for physics beyond the Standard Model. Likewise, atmospheric neutrinos can be used to study an ample variety of particle physics issues, such as neutrino oscillation phenomena, the determination of the neutrino mass ordering, non-standard neutrino interactions, neutrino decays and a diversity of other physics topics. In this article, we review a selected number of these topics, chosen on the basis of their scientific relevance and the involvement in their study of the Spanish physics community working in the KM3NeT and ANTARES neutrino telescopes.

Keywords: neutrino; neutrino telescopes; neutrino astrophysics; neutrino properties; sea science

1. Introduction

During the last decade, neutrino astronomy has enjoyed a true revolution following the detection of the first signals of very high-energy neutrinos [1] by the IceCube detector [2]. It has been a long way since the key concepts were proposed by M. Markov in 1961 [3]. Arriving at this point has required an enormous experimental effort and the determination and perseverance of hundreds of physicists and engineers. The potential to expand the harvest of scientific results in a variety of areas makes this endeavour worth pursuing. Several Spanish research groups have participated in the past and continue to participate at present in this worldwide undertaking through their work in the ANTARES [4] and KM3NeT [5] neutrino telescopes. In this article we review the contributions of the Spanish groups to these projects in the areas of design, construction, calibration, operation and physics analyses.

Neutrino telescopes have a very wide scientific scope. The rationale of these detectors stems from the fact that neutrinos are, at the same time, neutral, weakly-interacting particles and also the final, stable product of a variety of nuclear and particle physics processes.

This gives them a particular role in astronomy. The "traditional" messengers with which the Universe has been observed are photons and cosmic rays (CRs). They are abundantly produced in many sources and processes and are detected in a wide range of energies. However, they also suffer from several drawbacks. High energy photons (above a few TeV) are absorbed during their propagation from far sources. CRs, which are also absorbed at very high energies ($\gtrsim 5 \times 10^{19}$ eV), are deflected by Galactic and extra-galactic magnetic fields, which erase the information about their arrival direction. Neutrinos, on the contrary, can reach us unaltered. Therefore, neutrino astronomy is truly a novel way to observe the Universe. Not only they are almost ideal messengers, but they turn out to be copiously produced, as demonstrated by IceCube [6], resulting in an energy density comparable to that observed by Fermi-LAT in diffuse gamma rays [7] or by the Pierre Auger Observatory in ultra-high energy CRs [8]. However, there is an unavoidable challenge for neutrino astronomy: huge detectors are required given the small neutrino cross sections.

In addition to neutrino astronomy, there are other physics goals that these instruments can address, such as the search for dark matter and the study of neutrino properties, as discussed later on in this article. Finally, large arrays of sensors installed in the deep sea, like those deployed at the ANTARES or KM3NeT sites, also offer an opportunity to carry out oceanographic research.

The detection principle of neutrino telescopes is as follows. A large number of light detectors (photomultipliers encapsulated in pressure–resistant glass spheres, called "optical modules") are deployed in long lines which are installed in large volumes of transparent media (water in the sea or in lakes, ice in the Antarctica). These optical modules detect the Cherenkov light induced by charged particles produced in neutrino interactions with the matter within and around the detector. The current implementations of this idea are IceCube, in the South Pole; ANTARES and KM3NeT in the Mediterranean Sea, and Baikal-GVD [9] in the Baikal lake. The main background for cosmic neutrinos comes from the muons and neutrinos generated in the atmospheric showers produced in the interactions of CRs with the Earth's atmosphere. The flux of atmospheric muons is very large, but it can be drastically reduced by installing the detector deep in the water/ice and by selecting up-going events, since only neutrinos can traverse the Earth. The flux from atmospheric neutrinos is lower but comes from all directions. On the other hand, this source of atmospheric neutrinos represents a valuable opportunity for studies of neutrino oscillations, neutrino mass ordering and other fundamental neutrino properties.

Two main event topologies can be observed in these detectors: muon tracks and showers. Charged current interactions of muon neutrinos produce muons which can traverse long distances (hundreds of meters at high energy, $E \gtrsim 1$ TeV). This has two important advantages. First, it increases the effective volume of the detector. Second, it provides a very good angular resolution (about 0.1–0.3 degrees in water), thanks to the long lever-arm of these events. Neutral current interactions of any neutrino flavour and charged current interactions of electron and tau neutrinos produce showers which are seen as bright spheres. This topology has worse angular resolution and smaller effective volume, but a better energy resolution for contained events.

ANTARES is installed at a mooring depth of 2450 m in the Mediterranean Sea, close to the French coast, about 40 km off Toulon (see Figure 1, left). It consists of 12 vertical lines of a length of 450 m supporting a total of 885 optical modules. It was completed in 2008 and its decommissioning is planned for 2022.

KM3NeT is a distributed infrastructure composed of two detectors at two different locations: ARCA (offshore Portopalo, in the Sicilian coast) and ORCA (close to the ANTARES site). ARCA (Astronomy Research with Cosmics in the Abyss, see Figure 1, right) will consist of two blocks of 115 lines each with a total of about 4000 digital optical modules (DOMs). Every line (also called string or detector unit, DU) is 700 m high and has 18 DOMs, one every 36 m. Each DOM contains 31 3-inch photomultiplier tubes (PMTs). The horizontal distance between lines is about 90 m. ORCA (Oscillation Research with Cosmics in the Abyss) uses the same technology as ARCA, but with a denser configuration of DOMs.

The lines are 200 m high, with a vertical distance between DOMs of 9 m and a horizontal spacing between lines of roughly 23 m. It will consist of 115 lines with a total of about 2000 DOMs.

The difference in their geometry reflects the different physics goals for which they were designed. ORCA, being much denser, has a low energy threshold ($\sim$few GeV) which allows for studies on oscillations with atmospheric neutrinos. Its smaller size is compensated by the large fluxes at these energies (let us point out, though, that it will be much larger than some of the existing neutrino detectors in this energy range, such as SuperKamiokande). ARCA, on the contrary, offers a very large effective volume (about one cubic kilometer) which makes it appropriate for studying astrophysical neutrino fluxes at higher energies ($\gtrsim$100 GeV). This is not a strict separation and several of the physics studies benefit from both configurations, e.g., non-standard oscillation scenarios can be studied also at high energies, some astrophysical models predict signals at low energies, dark matter searches can take advantage of both ORCA and ARCA, etc.

At the time of this writing, 8 lines of ARCA and 10 lines of ORCA are installed and taking data.
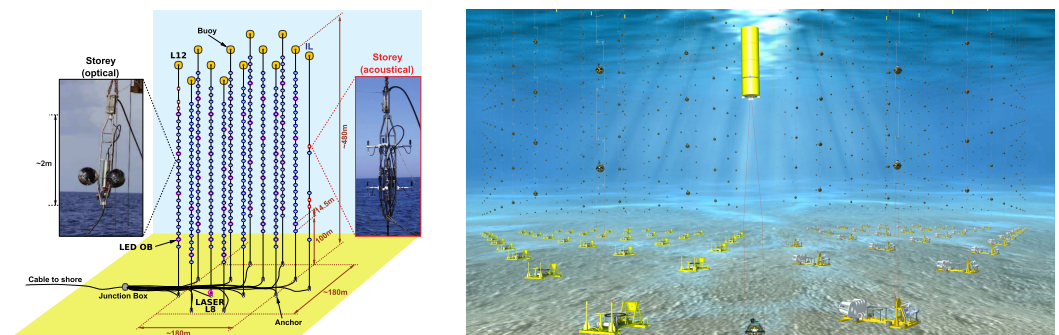
Figure 1. (**Left**) ANTARES schematics; (**Right**) Artist's impression of KM3NeT (credit: ANTARES and KM3NeT collaborations).

The involvement of Spain in neutrino telescopes started in 1997 when a team from IFIC (Instituto de Física Corpuscular, CSIC and University of Valencia), led by Juan José Hernández Rey, joined the ANTARES Collaboration. A few years later, other groups joined the project: IGIC (Institut d'Investigació per a la Gestió Integrada de les Zones Costaneres) from Universitat Politècnica de València (UPV) in 2006 and the University of Granada in 2015. In the mean time, the KM3NeT Collaboration was formed in 2006, including the Spanish groups. In addition, two marine science groups have also become members of KM3NeT: LAB (Laboratori d'Aplicacions Bioacústiques) from Universitat Politècnica de Catalunya (UPC) and Instituto Español de Oceanografía (C.N-IEO, CSIC). Recently, a group from the Institut de Ciències del Mar (ICM, CSIC) has joined KM3NeT as an observer member.

As will be discussed in this article, the contributions of the Spanish groups to ANTARES and KM3NeT along these years have covered many aspects of these projects. These contributions include, among others: the characterization of PMTs [10]; the design and construction of time and positioning calibration devices [11–17], acoustic instruments for R&D studies [18–20] and several contributions to electronics (the design and construction of electronic boards [21–25], the development of software and firmware and studies of electronics reliability [26,27]). On the physics side, the teams have participated in searches for neutrino point sources [28–36], diffuse fluxes [37,38], transient sources [39–41], multi-messenger astronomy [42–45], search for dark matter in the Sun [46–49] and in the Galactic Centre [50–55], searches for non-standard neutrino interactions [56–58] and neutrino decay [59].

We will review here a selection of some of these topics, grouped as follows: astronomy (Section 2), dark matter (Section 3), neutrino properties (Section 4), construction and calibration (Section 5) and sea science (Section 6).

2. Astrophysical Neutrinos

Cosmic Rays are ionized nuclei, mostly protons, of extraterrestrial origin that relentlessly strike the Earth with energies that go from a few GeV to several hundreds of EeV. The flux of CRs detected at Earth drops rapidly with the energy following a power law, $E^{-\gamma}$, with an index $\gamma \sim 3$. At low energies, below 10 GeV, CR production is dominated by the Sun. Then, up to PeV energies, it is commonly accepted that they are mainly produced by Galactic sources. These Galactic accelerators are unable to accelerate CRs above 10^{18} eV, therefore, CRs detected beyond those energies should be produced by extragalactic sources [60]. Identifying and studying those Galactic and extragalactic CR sources is one of the main goals of astroparticle physics. In order to search for them, one can use the reconstructed direction of the CRs detected at Earth and trace back their origin. However, since CRs are charged particles and travel through magnetic fields on their way to the Earth, their directionality is lost and the backtracking is not trivial. Only at ultra-high energies ($\gtrsim$few EeV) the particle trajectory is expected to be reconstructed with a sub-degree angular resolution. However, the statistics at those energies are small due to the low flux, and even large observatories, like Pierre Auger, have not been able to spot a clear detection of a high-energy CR source [61].

Apart from CRs, there are other messengers that have been proven to be valuable to study the most energetic phenomena in the Cosmos. These include gamma rays, gravitational waves (GWs) and neutrinos. Gamma rays of cosmic origin were first accidentally detected in the 1970s by military satellites [62]. Since then it has become clear that gamma-ray observation would be helpful to explore the Universe at high energies. Presently, several experiments, both Earth-based and in satellites, are operational and covering energy ranges that go up to PeV, with more than 200 sources known to be emitting in the TeV energy band or above [63].

GWs were theoretically predicted by Einstein at the beginning of the 20th century. Huge technological advances were required to build a detector sensitive enough to observe the first signal, in 2015, by the LIGO and Virgo collaborations [64]. Since operations started, GW observation has been very successful collecting relevant GW events (see for instance, Ref. [65]). Thanks to programmed detector upgrades and the recent addition of the KAGRA observatory [66], the next data taking run (O4), planned for late 2022, is expected to significantly increase both the statistics and the distance to which GW experiments are sensitive so far.

The last cosmic messenger in the list is the neutrino, the main subject of this review. As has been mentioned, the detection of neutrinos of astrophysical origin has been a major scientific goal of neutrino telescopes. The main advantage of neutrinos is that they are neutral, so unlike CRs they point back to the sources where they are produced. Also, the observation of neutrinos benefits from the fact that they are not absorbed by extragalactic background light, like gamma rays, or by the cosmic microwave background, like ultra-high energy CRs, and therefore the observable Universe at very high energies, above TeV, is not limited to nearby sources. On the other hand, the main disadvantage of neutrinos is that they have a small interaction cross section with matter and, as a result, large detection volumes are necessary to detect cosmic neutrino fluxes that, as it happens for CRs, steeply decrease with energy.

All four messengers described above complement each other since they are expected to be produced in common sources. A combined observation of several of these cosmic messengers in spatial and/or temporal coincidence outperforms significantly the discovery potential achieved by single messenger observations. This is the main idea of what has been coined as multi-messenger astronomy. For a recent review on multi-messenger astronomy with neutrinos see [67].

Focusing on neutrino astronomy, a major breakthrough came in 2013 with the discovery of a diffuse neutrino flux of cosmic origin by IceCube [6]. Independently, a hint of this diffuse flux (a 1.8σ excess) has also been observed with 12 years of ANTARES data [68]. Elucidating what are the sources of these high-energy neutrinos has been one of

the main research topics of the Spanish groups. As a matter of fact, the first search for point sources of cosmic neutrinos with ANTARES was done by Spanish scientists more than a decade ago [30] and they have been involved in this type of analysis ever since [31–34]. This includes collaboration between ANTARES and IceCube experiments, where the data of both detectors were used in a combined analysis [35], which was coordinated by the Spanish team.

In order to improve the sensitivity of these time integrated analyses, multiple transient correlations of CR source candidates have been studied, where the background is reduced under a time dependent neutrino emission hypothesis. In particular, the study of correlations in ANTARES with gamma-ray flares from blazars [39,40] and X-ray flares from X-ray binaries [41] have been carried out. The correlation of ANTARES neutrino candidates with IceCube high energy neutrino events was also evaluated [42].

Up to now all these searches have been unsuccessful. However, there are good reasons to believe that the next generation experiments, like KM3NeT, should be sensitive enough to finally provide a clear detection of a cosmic neutrino source above the 5σ discovery threshold. For instance, the most recent analyses using IceCube [69] and/or ANTARES data [28,36] have found promising candidates with an statistical excess close to 3σ. The differential energy flux sensitivities of current experiments as a function of the sine of the declination, δ, together with the one expected for KM3NeT, are illustrated in Figure 2. The most recent sky map produced with ANTARES data with a livetime of 13 years is displayed in Figure 3.
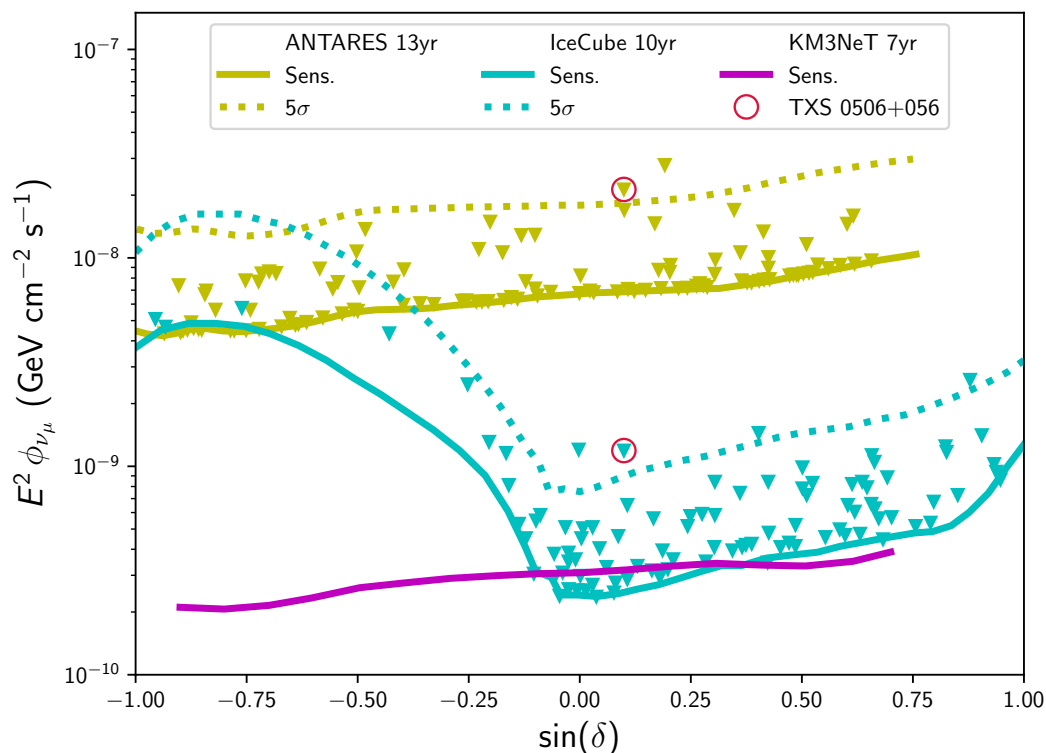
Figure 2. Differential energy flux sensitivity curves as a function of the sine of the declination, δ, from current neutrino telescopes: ANTARES [28], IceCube [69] and KM3NeT [70], with flux upper limits for individual source candidates (triangles) in ANTARES and IceCube. Notice that the sensitivity of KM3NeT is obtained assuming a fully operational detector. Differences in curve shapes depend mostly on detector latitudes due to the dominant event topologies (muon tracks) and backgrounds in play (e.g., atmospheric muons).
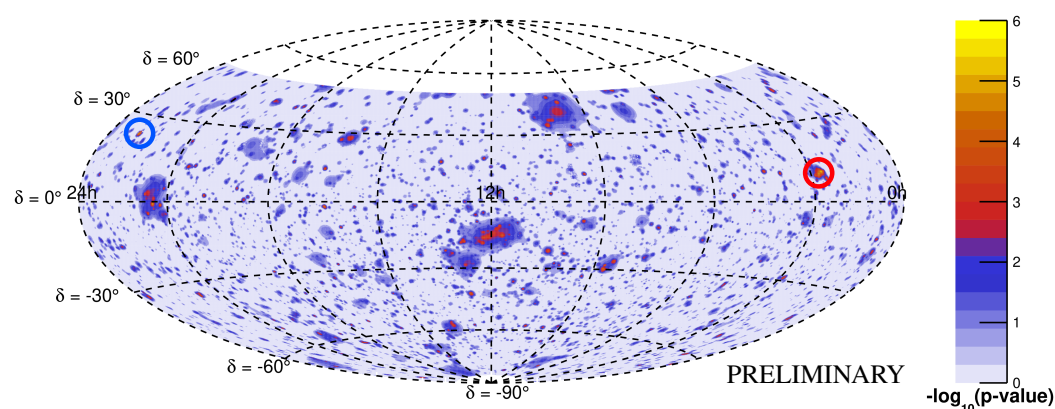
Figure 3. Sky map in equatorial coordinates of pre-trial *p*-values for point-like sources of the ANTARES visible sky (declination, *δ*, in degrees; right ascension in hours). The location of the most (second most) significant cluster of the full-sky search is indicated by the red (blue) circle. Figure adapted from Ref. [28].

At the moment, the most compelling evidence of a candidate neutrino source came from the combined detection of a high-energy neutrino from IceCube (IceCube-170922A) in spatial coincidence with a blazar (TXS 0506+056). When the neutrino was detected, a flare in gamma rays was observed by the Fermi-LAT satellite. This coincident event was discarded to be a background fluctuation at the 3σ level [71]. Moreover, after this event was detected, a dedicated analysis including archival data from IceCube was performed unveiling a flare of neutrinos between September 2014 and March 2015 with 3.5σ statistical significance [72]. In this case, the associated blazar was not observed in a gamma-ray flare emission state. This event is an example of the potential of multi-messenger astronomy, where the spatial and/or temporal simultaneous observation of different cosmic messengers helped identify a potential CR source.

Even if the ANTARES detector has a lower sensitivity compared to IceCube, the blazar TXS 0506+056 appeared as the second most significant excess (2.8σ pre-trial) in a search using a list of 121 pre-selected sources [28]. This result supports the hypothesis of TXS 0506+056 being a genuine cosmic neutrino source. Time-independent and time-dependent analyses were also performed right after the announcement of this historic event [43].

Despite the fact that dedicated analyses and follow-up campaigns have been carried out, it is still unclear how neutrinos are produced in blazars and how much they contribute to the total neutrino diffuse flux (see Ref. [73] for an updated review). One of the hypotheses that has risen in popularity lately is the multi-zone model, where neutrinos and gamma rays would be produced in different regions in the source. Connected to this, it has recently been discovered a convincing link between neutrinos and radio blazars [74], suggesting that X-ray and radio emission may be better correlated with neutrino emission. This reinforces the idea of neutrinos and gamma rays being produced in different regions [75]. The correlation with radio blazars is also supported by ANTARES observations [76]. In this sense, one of the most recent analyses performed by the collaboration reported a very interesting association coming from PKS 0239+108 [77].

Among the candidates postulated as cosmic neutrino sources, Tidal Disruption Events (TDEs) have got particular attention in recent years thanks to a possible coincidence with an IceCube neutrino [78]. TDEs are produced when a star passes very close to a massive black hole, which tears the star apart with a corresponding electromagnetic emission. In the process, neutrino production is also expected (see, for instance, Ref. [79]). The TDE-neutrino coincidence was not correlated in time. However, since TDE events are infrequent, the calculated coincidence probability of having such an event should be less than 0.5%. In addition to that event, another TDE was also found more recently in coincidence with a different neutrino event [80]. Both TDE-neutrino events were checked using data from

ANTARES. However, no significant correlation was found [81]. Nevertheless, the non detection by ANTARES is still compatible with the neutrino flux estimated from the TDEs.

Other candidates postulated to emit cosmic neutrinos are Gamma-Ray Bursts (GRBs) [82]. GRBs are episodic events that are closely related to GWs. For some cases, like neutron star mergers, a neutrino flux is expected [83]. A particular example is the multi-messenger detection that took place in August 2017, when a GW event (GW170817) was detected in spatial and temporal coincidence with GRB 170817A, triggering a multi-collaboration wide study [84]. Although no significant neutrino emission was detected from this event, the prospects for future neutrino detectors are that they should be sensitive enough to observe some of these events in several optimistic scenarios, as shown in Figure 4. Likewise, estimates of the potential of KM3NeT to detect the low energy neutrinos from core-collapse supernovae, closely related to long GRB events, have been performed [85,86].
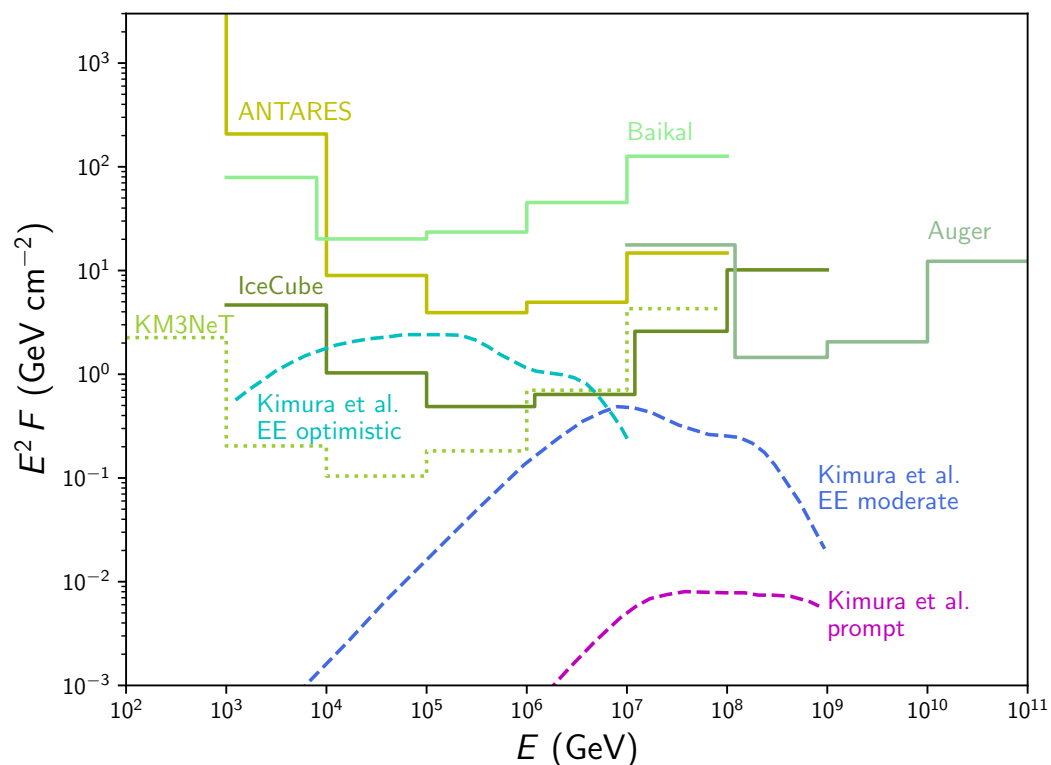
Figure 4. Fluence upper limits per flavour on the high-energy neutrino emission from experimental data assuming a ± 500 s time window around the GW170817 event [87]. Baikal limits are from Ref. [88]. KM3NeT preliminary sensitivity, computed for an optimal zenith angle, is from Ref. [44]. Theoretical models for comparison are from Ref. [83]. Figure taken from Ref. [67].

Given their potential as neutrino emitters, follow-up observations of the most important GRB and GW events have been performed with neutrino telescopes, for instance by ANTARES for GW170817 [87] and GW170104 [89]. However, no significant excess has been found so far. In the case of ANTARES the latest results can be found in Refs. [90,91]. A similar analysis technique was used to follow up a list of interesting events triggered by other experiments, e.g., the three most significant events observed by Baikal-GVD were checked using ANTARES data [45].

Concerning our cosmic neighbourhood, particle accelerators hosted in the Galaxy should be energetic enough to accelerate particles up to PeV energies. High-energy neutrinos are expected to be produced and accelerated in those sources if hadronic processes are taking place. As a matter of fact, thanks to recent gamma-ray observations there are hints of such processes both in point sources [92] and diffuse emission [93]. The case of ANTARES and KM3NeT detectors are of special relevance, as both are very well located

to observe the inner part of the Galaxy. Even if no significant detection were observed in ANTARES, either as point-like [28] or diffuse [94,95] sources, the odds are much better with a telescope as large as KM3NeT, for which current models predict that its sensitivity will be good enough to detect the several Galactic candidates suggested by gamma-ray observatories [96].

3. Searching for Dark Matter

Besides astrophysical messengers, neutrinos can also be tracers of the annihilation or decay of dark matter particles [97]. The possible existence of dark matter (DM) hinted by its gravitational effects calls for a search of new elementary particles that may explain the observations: rotation curves of galaxies and galaxy clusters, gravitational lensing and cosmology. However, all attempts to identify a fundamental component of dark matter have yielded no positive result yet. Elementary dark matter particles are difficult to detect due to their weak interaction with ordinary matter. In some scenarios, they would accumulate in massive astrophysical objects due to gravitation. In order to enhance the possibility of observing them despite their low interaction rates, detectors target accumulation sites in astrophysical environments. Such dark matter sources, considerably spatially extended with respect to classical astrophysical emitters, carry a dark matter content that is usually described by the J-factor:

$$J_{\text{ann}} = \int_{\Omega} d\Omega \int_{l} \rho^2(r(\theta, \phi)) dl \ \text{ or } \ J_{\text{dec}} = \int_{\Omega} d\Omega \int_{l} \rho(r(\theta, \phi)) dl \tag{1}$$

(for annihilation and decay, respectively) expressing the dark matter density integrated over a viewing angle Ω along the line of sight l. The shape of the dark matter halo $\rho(r(\theta, \phi))$ is, in turn, described with models based on astrophysical data, or taking input from N-body simulations. Indirect dark matter searches using neutrinos as a byproduct of dark matter annihilation or decay are usually restricted to WIMP scenarios, which posit a general class of *weakly interacting massive particles* (WIMPs), whose interaction strength is of the same order of magnitude as the known Standard Model weak interaction. In this framework, there are tools that enable the evaluation of the neutrino yield produced in pair annihilation or decay of dark matter particles, in terms of the number of outgoing secondaries per unit of energy. In indirect searches, a neutrino telescope performs a measurement of the outgoing event rate from a process such as:

$$\text{WIMP WIMP} \xrightarrow{\text{ann}} \text{intermediate channel(IC)} \rightarrow \nu\bar{\nu} \ \text{ or } \ \text{WIMP} \xrightarrow{\text{dec}} \text{IC} \rightarrow \nu\bar{\nu}. \tag{2}$$

WIMP particles are usually assumed to range in mass from a $\mathcal{O}(\text{GeV})$ to $\mathcal{O}(100 \text{ TeV})$, and move non-relativistically. In the case of dark matter decay, if no hint is found, limits can be placed on the particle lifetime. For dark matter pair annihilation, it is possible in general to translate the limit on the number of collisions to a limit on the annihilation cross section. Moreover, if the astrophysical object studied has a known chemical composition (for instance, in the case of the Sun as a dark matter source) this limit can be translated into a limit on the spin-dependent and spin-independent cross section for WIMP-nucleon interaction.

To perform a search for dark matter in data collected by neutrino telescopes, the basic information used is the neutrino direction and energy inferred from the neutrino-induced events. These searches are typically structured as hypothesis tests. A signal hypothesis, in which a cluster of neutrino events around the source region is assumed to come from dark-matter pair annihilation, is confronted to the null hypothesis where all events in the sample are neutrinos originated in the Earth's atmosphere. A Monte Carlo set of neutrino events permits to simulate the space and energy distribution of the dark matter signal, whilst the background description is usually obtained from data shuffled in right ascension.

Since the possible mass of the dark matter particle—and thus the corresponding neutrino energy—span a large range of values, the search should be performed with all the detectors under consideration here: ANTARES and KM3NeT (ORCA and ARCA). A variety of analyses looking for dark matter have been carried out [46–48,51,52]. A highlight result

is obtained searching in the Galactic Centre region, which is the most promising source due to its expected dark matter content, being at once dense in dark matter and relatively close to the Earth, which translates into the highest J-factor. Moreover, the Galactic Centre has an excellent visibility from the location of Mediterranean telescopes, with an uptime of about 70%. ANTARES currently has world-leading limits for those dark matter annihilation channels exclusively visible with neutrinos. Figure 5 shows the results for a benchmark channel ($\tau^+\tau^-$) for both neutrinos and γ-rays as particle tracer. Limits placed by IceCube are much less stringent (in particular at large masses) due to the fact that the Galactic Centre is above the horizon for this detector, i.e., in a region with huge background from atmospheric muons. The sensitivity at reach with one year of ARCA in its full configuration is shown along with the limits produced by ANTARES in 14 years of data [52].
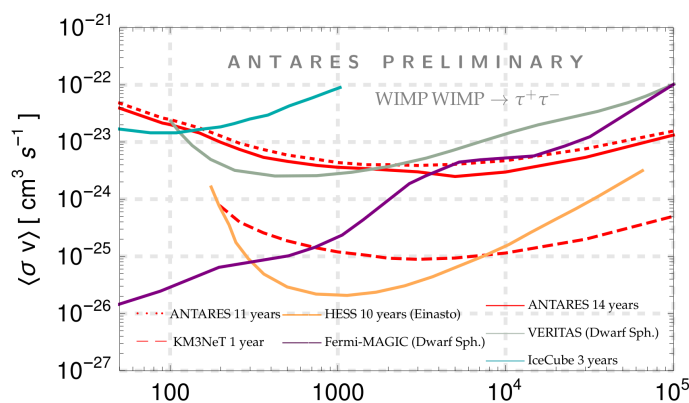

Figure 5. Upper limits at 90% CL on the thermally averaged cross section for WIMP pair annihilation as a function of the WIMP candidate mass set with 14 years of ANTARES data [52], in comparison with the measurement from IceCube [98], H.E.S.S. [99], VERITAS [100] and Fermi-LAT+MAGIC [101], for the $\tau^+\tau^-$ channel and NFW dark matter halo [102], unless specified. The sensitivity that could be reached with KM3NeT in one year is shown in dashed red. Credit: ANTARES and KM3NeT Collaborations.

The good visibility of the Galactic Centre from the Mediterranean Sea is exploited by ANTARES for other dark matter searches. A combined ANTARES and IceCube search for WIMPs from the Galactic Centre region in the GeV–TeV energy range has been performed [53]. In this region of the mass spectrum the sensitivities of ANTARES and IceCube are comparable: although IceCube has a much larger instrumented volume, its sensitive volume must be reduced to its inner core, using the outer layers as a veto to suppress the atmospheric muon background. ANTARES and IceCube have improved upon their standalone limits up to a factor of 2 combining their data sets into a joined likelihood search, as shown in Figure 6. Exploratory searches for annihilations of heavy dark matter in secluded scenarios [103], where the two dark matter particles are isolated from their Standard Model products by an on-shell mediator, have also been performed by ANTARES. This new particle modifies the cosmological freeze-out point allowing for the computation of annihilation rates of dark matter well above the TeV scale, in line with recent searches at colliders. The results obtained with ANTARES set limits for the first time up to 6 PeV in energy [55]. The first search for secluded DM in neutrino telescopes was also led by us, but for lower DM masses and looking at the Sun with ANTARES [47]. Later, the UPV group also looked for secluded dark matter using public data of Icecube [104].
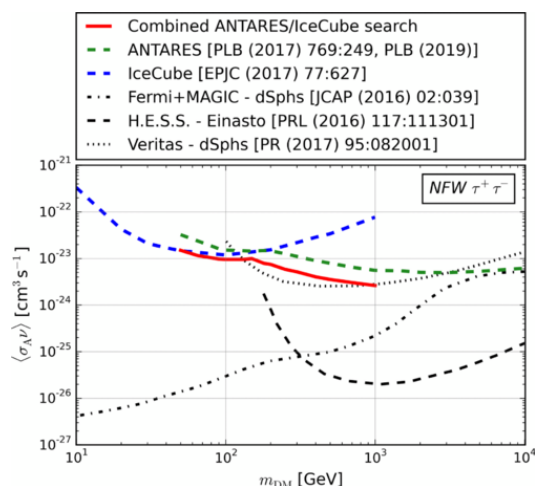
Figure 6. 90% CL upper limit on the thermally-averaged dark matter annihilation cross section $<\sigma_A \cdot v>$ obtained for the combined analysis as a function of the dark matter mass m_{DM} assuming the NFW halo profile for the $\tau^+ \tau^-$ annihilation channel [53]. The limits from IceCube [98], ANTARES [52], VERITAS [100], Fermi+MAGIC [101] and H.E.S.S. [99] are also shown.

Indirect searches for dark matter from the Sun with the ANTARES and ORCA detectors have been also carried out. Even though spin-dependent interactions with hydrogen atoms are expected to dominate (due to the large abundance of this element in the star), spin-independent WIMP interactions with heavier nuclei, like helium or oxygen, are also possible. The search, focused on track-like events, uses a strategy based on the maximisation of a likelihood function with information on the characteristics of signal and background events. The resulting cross-section limits are shown in Figure 7, together with the results of other experiments for the sake of comparison.
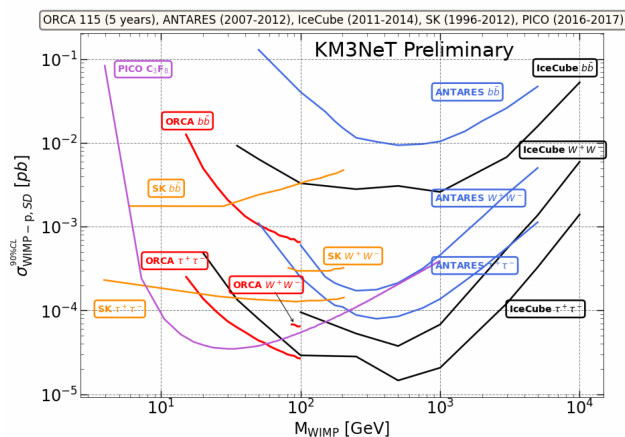
Figure 7. Limits on the WIMP-proton spin-dependent scattering cross sections as a function of the WIMP mass for ANTARES (5 years [48]) and ORCA (5 years of simulated data [49]). Limits from Ice Cube [98], Super Kamiokande [105] and PICO [106] are also shown for comparison. Credit: ANTARES and KM3NeT Collaborations.

An unavoidable background for these dark matter searches comes from Solar Atmospheric Neutrinos (SAνs). A flux of high energy (GeV to PeV) neutrinos is expected from the Sun direction, originating from the decay of the particles produced by CRs interacting in the Sun [107]. The sensitivity of current experiments is not yet large enough to detect this neutrino flux. Besides the importance of understanding the characteristics of this potential background source, the detection of these SAνs can help better understand the solar density and shed light on the primary CR composition [108,109]. Recently, SAνs have been searched for with the ANTARES detector using 11 years of data (2008–2018) [109].

Several CR models as signal component [110,111], different solar density profiles [112,113] and source shapes (the Sun as a point source, as a filled disk or with ring shape) were tested. The analysis is based on an unbinned likelihood that considers only the track channel, taking advantage of the excellent ANTARES angular resolution. No evidence for a signal over the expected background was observed. Assuming as baseline models those of Refs. [110,112], a 90% CL upper limit on the energy flux of about 7×10^{-11} TeV cm^{-2} s^{-1} was established at $E_\nu = 1$ TeV.

4. Neutrino Physics and Search for New Physics

ANTARES and KM3NeT are excellent tools to probe neutrino physics using atmospheric neutrinos. ORCA was designed with the main goal of determining the neutrino mass ordering through atmospheric neutrinos, but new particles or phenomena can be looked for with these neutrinos, such as heavy neutral leptons or sterile neutrinos, non-standard neutrino interactions, neutrino decay, Lorentz invariance violation or neutrino decoherence.

Physics Beyond the Standard Model can be tackled in a model-independent way by means of effective field theory (EFT). In EFT, the influence at low energy of potential new physics at a higher energy scale is described by sums of non-renormalisable operators built from the fields at the lower scale. It is possible to construct a wide variety of these beyond the Standard Model (BSM) operators for neutrinos [114], but traditionally the term "non-standard interactions" (NSIs) [115,116] has designated a subset of this BSM interactions corresponding to four-fermion interactions described by dimension six operators of the form:

$$\mathcal{L}_{\text{NSI}}^{\text{CC}} = -2\sqrt{2}G_F \sum_{ff'X} \varepsilon_{\alpha\beta}^{ff'\,X} \left(\bar{\nu}_\alpha \gamma^\mu P_L l_\beta\right) \left(\bar{f} \gamma_\mu P_X f'\right) \tag{3}$$

$$\mathcal{L}_{\text{NSI}}^{\text{NC}} = -2\sqrt{2}G_F \sum_{fX} \varepsilon_{\alpha\beta}^{f\,X} \left(\bar{\nu}_\alpha \gamma^\mu P_L \nu_\beta\right) \left(\bar{f} \gamma_\mu P_X f\right), \tag{4}$$

where G_F is the Fermi constant, P_X (with $X = R$ or L) denotes the chiral projection operators $P_{R,L} = \frac{1}{2}\left(1 \pm \gamma^5\right)$, f is a first generation SM fermion (e, u or d-quarks), f' belongs to the same weak doublet as f, and α and β denote the neutrino flavours: e, μ or τ. The dimensionless coefficients $\varepsilon_{\alpha\beta}^{ff'\,X}$ and $\varepsilon_{\alpha\beta}^{f\,X}$ quantify the strength of NSIs between the neutrinos of flavour α and β and the matter fermion $f \in \{e, u \text{ or } d\}$ (for neutral currents) and $f \neq f' \in \{u,d\}$ (for charged currents). The standard oscillations scenario is recovered in the limit $\varepsilon \to 0$.

Charged current (CC) NSIs affect the production and detection processes, while neutral current (NC) NSIs would influence the neutrino propagation by coherent forward scattering of neutrinos with matter. In the case of atmospheric neutrinos, this scattering will modify the Standard Model potential that describes the matter effects in neutrino flavour oscillations, giving rise to additional effects that will deviate from the conventional expectations for the oscillation phenomena in matter [116–120].

The existence of NSIs can be described as a new potential that will translate into an additional term in the Hamiltonian:

$$H^{\text{NSI}} = V_{CC} \frac{n_f}{n_e} \varepsilon, \tag{5}$$

where n_f and n_e are the fermion and electron number density along the neutrino path. For simplicity, neutrinos are assumed to interact with down quarks which, for the case of the Earth, are roughly three times as abundant as electrons, $n_f = n_d \approx 3 \, n_e$. The matrix ε ($\varepsilon_{\alpha\beta}$, α, β = e, μ, τ) gives the strength of the NSI. Its diagonal terms, if different from each other, can give rise to the violation of leptonic universality, while the off-diagonal terms can induce flavour changing neutral currents, which are highly suppressed in the SM. Taking into account the hermiticity of the Hamiltonian and the fact that it can only be determined by oscillation experiments up to an overall multiple of the identity matrix, there

are 8 NSI real parameters, namely [121]: two free real parameters in the diagonal and three off-diagonal complex parameters, i.e. three moduli plus three phases. The undetermined parameter in the diagonal is customarily taken into account subtracting $\varepsilon_{\mu\mu}$ from the rest, so that the diagonal reads: diag($1 + \varepsilon_{ee} - \varepsilon_{\mu\mu}$, 0, $\varepsilon_{\tau\tau} - \varepsilon_{\mu\mu}$). In this paper we assume $\varepsilon_{\tau\tau}$ to be already referred to $\varepsilon_{\mu\mu}$, or equivalently, we consider $\varepsilon_{\mu\mu}$ to be zero.

The search for possible indications of NSIs is being performed using the data recorded by ANTARES from 2007 to 2016 (both years included), corresponding to a total livetime of 2830 days. From this recorded data, a final sample of 7710 reconstructed events were selected, which was used to perform a muon neutrino disappearance study that provided a measurement of the oscillation parameters Δm^2_{32} and θ_{23} and established limits to the possible existence of an additional sterile neutrino family [122]. Possible NSI effects were looked for making some simplifying assumptions. Since ANTARES is largely sensitive to the ν_μ disappearance channel, it can probe the NSI parameters $\varepsilon_{\tau\tau}$ and $\varepsilon_{\mu\tau}$, which are considered in this search to be both real-valued parameters. A likelihood ratio method has been used that includes, in addition to the two NSI parameters, another eight free nuisance parameters that take into account the uncertainties in the knowledge of the four oscillation parameters Δm^2_{31}, θ_{23}, θ_{13} and δ_{CP}, and in another four parameters related to the atmospheric neutrino flux, such as its global normalisation, its spectral index, the neutrino-antineutrino flux ratio and the models that describe neutrino interactions.

Preliminary results [57] indicate that the data are consistent with standard oscillations at the 1.8σ level. In Figure 8 the contours of 90% CL in the $\varepsilon_{\mu\tau} - \varepsilon_{\tau\tau}$ plane are shown assuming normal ordering of neutrino masses.
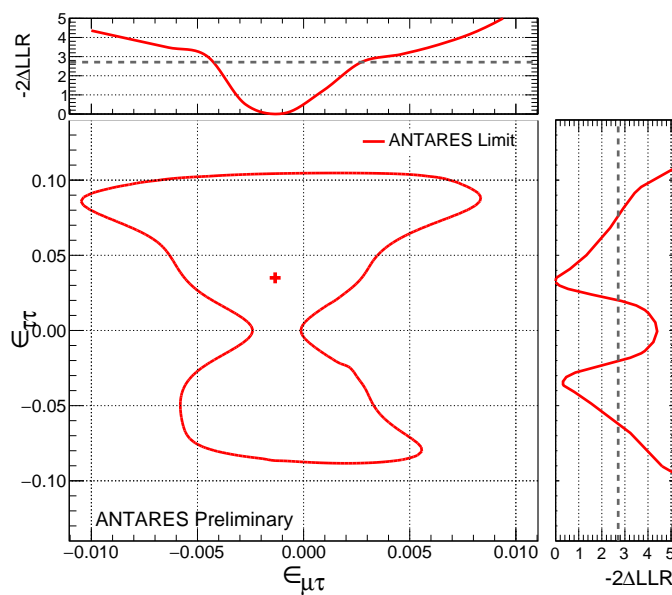
Figure 8. Contours of 90% confidence level on the $\varepsilon_{\mu\tau} - \varepsilon_{\tau\tau}$ plane, after 10 years of ANTARES data. The cross indicates the best-fit point. The top and right lateral plots show the 1D profile likelihood of the respective NSI parameter when the other parameter is fitted over. The dashed straight lines indicate the 90% CL value for one degree of freedom. Credit: ANTARES Collaboration.

The top and right one-dimensional plots show the profiled distributions in each of the two parameters from which it can inferred that $-4.2 \times 10^{-3} < \varepsilon_{\mu\tau} < 2.7 \times 10^{-3}$ and that $(-6.1 \times 10^{-2} < \varepsilon_{\tau\tau} < -2.1 \times 10^{-2}) \cup (2.1 \times 10^{-2} < \varepsilon_{\tau\tau} < 7.3 \times 10^{-2})$ at the 90% confidence level.

The best-fit value for ($\varepsilon_{\tau\tau}, \varepsilon_{\mu\tau}$) is different from zero at the 1.7σ level assuming normal mass ordering (besides inverting the sign of the corresponding parameter, the influence of the neutrino mass ordering on these results is in general small). Separately, the best-fit value of $\varepsilon_{\mu\tau}$ is compatible with zero within errors. However, $\varepsilon_{\tau\tau}$ is compatible with zero

only within its 95% CL range. These limits are slightly more stringent than those obtained by other neutrino telescopes such as SuperKamiokande [123] and IceCube [124].

A prospective study of the reach of the ORCA detector has also been performed [57,58]. In this case the NSI parameters $\varepsilon_{e\mu}$, $\varepsilon_{e\tau}$, $\varepsilon_{\mu\tau}$ and $\varepsilon_{\tau\tau}$ have been studied and the results indicate that with three years of data taking, ORCA can constraint these parameters with bounds one order of magnitude better than present limits. The limits obtained at the 90% CL for the absolute values of $\varepsilon_{e\mu}$, $\varepsilon_{e\tau}$ and $\varepsilon_{\tau\tau}$ are around 10^{-2} and go down to 10^{-3} for $\varepsilon_{\mu\tau}$.

The ORCA detector is at present being deployed under the Mediterranean Sea. A version with six lines has been taking data since more than one year. A preliminary study [56] restricted to the $\varepsilon_{\mu\tau}$ parameter shows that the sensitivity is just a factor 4 worse than the current best limits, i.e limits around 10^{-2} for this parameter could be achieved with such a small detector (5% of the full ORCA) and with just one year of data. The analysis with real data is ongoing and results will be soon obtained.

A different BSM scenario that can alter the pattern of neutrino oscillations is the unstable neutrino hypothesis. Neutrino decay models depend on whether the neutrino is a Majorana or a Dirac particle. For Majorana neutrinos there are models in which a neutrino, ν_i, can decay into another lighter neutrino, ν_j, and a new boson, J, called Majoron [125], $\nu_i \rightarrow \nu_j + J$. If neutrinos are Dirac particles, they can decay through the reaction $\nu_{iL} \rightarrow \nu_{iR} + \chi$ into an iso-singlet and a right-handed neutrino [126]. Depending on whether the final neutrino state is active or not, decay models are classified as visible or invisible, respectively. In the approach followed in ORCA, the heaviest mass eigenstate, ν_3, decays to a new fourth mass state, ν_4, which is assumed to be sterile and remains unobserved. This means that this new state cannot mix with the other active neutrino states and, therefore, does not oscillate.

Phenomenologically, the neutrino decay is taken into account by modifying the Hamiltonian including a decay constant $\alpha_3 = m_3/\tau_3$, where m_3 is the mass of the third mass state and τ_3 is its rest-frame lifetime. The introduction of a decay constant makes the mixing matrix non Hermitian and, therefore, the sum of the oscillation probabilities becomes lower than one: $P_{\alpha e} + P_{\alpha\mu} + P_{\alpha\tau} < 1$.

As a consequence of the neutrino decay, there is a global decrease in the probabilities and a damping effect on the atmospheric oscillation pattern. These effects are most notable in the range of zenith angles and energies close to the matter effect resonance, the 3–8 GeV region. The sensitivity of ORCA to neutrino decay was first estimated in [59] showing that bounds on the decay constant could improve those from current experiments by a factor 100. After ten years of data taking with the full ORCA detector, the sensitivity would be $\tau_3/m_3 = 2.5 \times 10^{-10}$ s/eV at 90 % CL. More realistic studies being carried out currently by the ORCA collaboration show slightly lower values but still of the same order of magnitude. On the other hand, preliminary results obtained from the first 6 lines deployed in ORCA provide bounds very close to the present limits from other experiments.

5. Design and Instrumentation of the Detectors

ANTARES and KM3NeT have been possible after an extensive design, test and construction program in which the Spanish groups have actively participated. This work still continues for the case of KM3NeT. The main activities in which the Spanish groups have contributed are summarised in this section.

5.1. Time Calibration Instrumentation for Neutrino Telescopes

Time calibration is crucial in neutrino telescopes since it is directly related to the accuracy in the angular reconstruction, a key performance parameter for such instruments. Several complementary techniques are used prior to the installation of the lines and in situ after their deployment. Among the latter, we can use the light from calibration sources (the so-called "optical beacons"), potassium-40 decays (naturally present in the water) or from atmospheric muons.

In ANTARES, there are two kinds of optical beacons [11]: the laser beacon and the LED beacons.

The laser beacon emits very intense, fast light pulses (of the order of a nanosecond), which can reach longer distances than the LED beacons. For this reason, its main application in ANTARES has been for calibration between lines, since the photons emitted by the laser installed at the base of a line are able to reach adjacent lines.

The laser beacon was developed for ANTARES [14] by the Spanish groups (see Figure 9, left). A Nd–YAG laser (Q-switch, pulsed pumped diode) was chosen, which provides pulses with a duration of 400 ps (FWHM) with a total energy of 3.5 µJ. The emission wavelength is 532 nm. In order to vary the amount of emitted light, a voltage controlled attenuator was added. This attenuator uses a variable liquid-crystal retarder located in the path of the laser beam. The laser and its associated electronics is housed in a titanium container capable of withstanding pressures up to 3500 m depth.

The light pulses of the LED beacons are wider than those of the laser beacon, about 4–5 ns (FWHM) with a rise time of 2–3 ns. The wavelength emission is 470 nm. The pulser circuit is based on the Kapustinsky circuit [127], in which two interconnected transistors generate the electrical pulse that stimulates the LED during the transition from open to closed and back. In this way, a very narrow electrical pulse is achieved, which in turn generates an optical pulse with a similar duration. In ANTARES, a LED beacon is made up of 36 LEDs and their corresponding pulser circuits, distributed on six boards forming a hexagonal prism (see Figure 9, right).
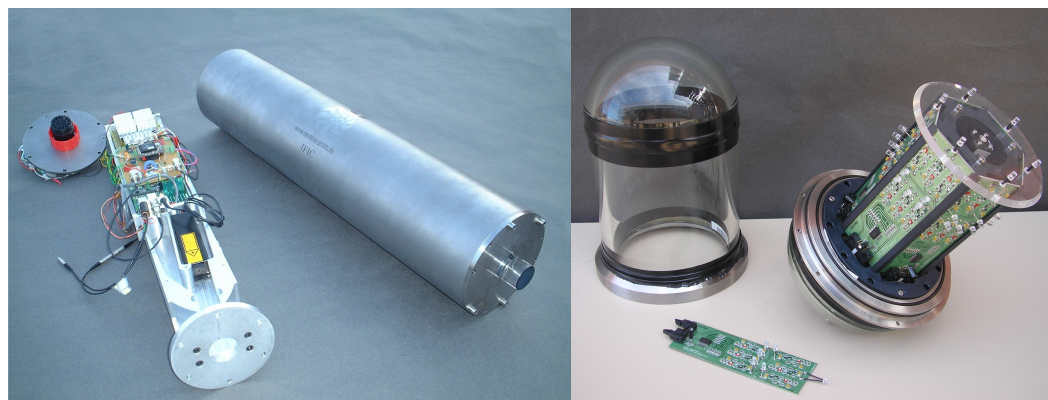

Figure 9. Detail of the laser beacon with the laser head, the power supply and the electronic control system (**left**) and LED optical beacon with its cylindrical pressure-resistant glass vessel (**right**).

The same model of laser beacon has been proposed for KM3NeT, studying the possibility of using more intense light sources. For its validation, two prototypes were installed both in ANTARES and in the NEMO towers [128,129]. Based on the previous experience of ANTARES and in order to reduce the cost and power consumption, the LED beacons were replaced in KM3NeT by the so-called nanobeacons, installed in each DOM [15,16] (see Figure 10). The pulser circuit has been miniaturised reducing it to a single LED diode, integrated into the DOM and pointing upwards to other DOMs on the same line. This avoids the use of a container and its interconnection cables. The nanobeacon electronics consist of two components: the pulser circuitry and the control electronics [130].

5.2. KM3NeT Acquisition Electronics

The Spanish groups had a leading role in the design of the KM3NeT acquisition and control electronics [131–135]. They had a deep involvement in the Central Logic Board (CLB) and the Power Board (PB), and have coordinated the design, prototyping, testing, and commissioning of the overall system. The location of the acquisition electronic boards inside the DOM is shown in Figure 10.
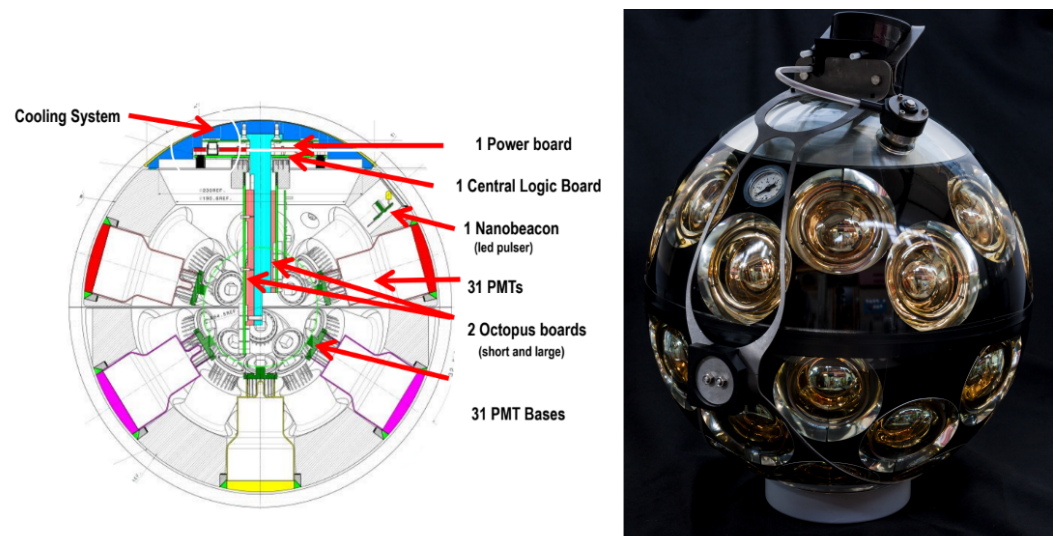
Figure 10. (**Left**) Scheme of a Digital Optical Module with the location of the acquisition electronics; (**Right**) Picture of a completed DOM. Credits: KM3NeT.

The PB provides power to the entire DOM, including the PMTs, the acquisition electronics and the instrumentation. A 12 V input coming from outside the DOM supplies the PB. Six regulated voltages are generated from this input using DC/DC converters. The PB is located in the shielded part of the heat-sink, which, in addition to providing cooling to this board, isolates the DOM from high-frequency interferences. Another function of the PB is to provide the startup sequence of the FPGA voltages. For this purpose, the PB incorporates a sequencer. The PB also includes a hysteresis loop that prevents instabilities during startup. The PB regulators are activated only when the input voltage exceeds 11 V, while they deactivate when the input value falls below 9.5 V. This prevents fluctuations in the PB regulators.

The Central Logic Board (CLB) is the main electronic board of the KM3NeT acquisition system [21,23,24,136]. The LVDS signals from the PMT base are digitised by the TDCs implemented in the FPGA with a resolution of one nanosecond. After organising and adding the arrival timestamp of the signals, the data acquired by the TDCs are sent to the shore control station for further process and storage. The CLB also incorporates a compass and an inclinometer, three temperature sensors and a humidity sensor. The control of the CLB is achieved through a processor embedded in the FPGA programmable logic of the CLB. The main component of the CLB is the FPGA, from the Xilinx Kintex-7 family, chosen for its relatively low power consumption. Other relevant components are a flash memory, which communicates via SPI with the FPGA and stores four of the FPGA images together with the CLB configuration parameters and programmable oscillators, which provide the clock signals required by the White Rabbit protocol [137]. The main element to communicate with the shore control station is the SFP transceiver, which interfaces the electronics with the optical system. The firmware runs on the CLB FPGA, being its main components: the embedded LM32 processor, on which the CLB control and monitoring software runs; the White Rabbit PTP core, which implements the White Rabbit protocol; the TDCs, which digitise the PMT signals that arrive at the CLB; the state machine and the multiboot core, which allows the secure remote configuration of the FPGA firmware.

5.3. Reliability

The maintenance of the detection lines installed at the bottom of the sea is very difficult, if not unfeasible, so a high level of reliability is required to guarantee the correct functioning of the electronics during the experiment's lifetime. To quantify the reliability of the KM3NeT electronics acquisition system, the FIDES method has been used [26,27,138]. This method has been applied to the acquisition system boards, obtaining the Mean Time

To Failure (MTTF) from them. Table 1 shows the MTTF values obtained for the main electronics boards of the KM3NeT DOM.

Table 1. Mean Time to Failure expressed in million of hours for CLB, PB and the main DC/DC converter within the DOM. These calculations mean if we would have one single DOM, it would have a failure every 0.7 million of hours.

Board	MTTF (Million of Hours)
CLB	2.8
PB	1.5
DC/DC converter	2.5
Overall	0.7

By means of the MTTF, it is possible to calculate the so-called reliability function,

$$R(t) = e^{-t/\tau} \tag{6}$$

where τ is the MTTF and t is the number of hours. This equation represents the probability that a system has worked up to a certain time without failure. This means, for instance, that 88% of the DOMs will not have any failure in the first 10 years of the KM3NeT experiment.

5.4. KM3NeT Positioning System

The KM3NeT detector lines are held vertically by buoyancy and can slightly move under the influence of the sea currents. To properly reconstruct the direction of the incoming neutrino, the position of the DOMs must be known with an accuracy better than 10 cm. To this aim, the DOMs are instrumented with acoustic and orientation sensors. The UPV group has significantly contributed to the design of the system and on the instrumentation involved, as well as in the development of the prototype instrumentation, and in the operation and analysis of the data of these systems both in ANTARES and KM3NeT [17,139–142].

The acoustic positioning system (APS) is used to determine the position of the DOMs. Using signals emitted from the acoustic beacons anchored on the seabed in known fixed locations, the position of the acoustic receivers are determined by the trilateration method. These receivers consist of piezoceramic sensors installed inside the glass sphere and hydrophones in the base of the DU. The data recorded by the receivers are analysed by the Acoustic Data Filter, searching for the signals, via the cross-correlation method, and registering the time of arrival used for the trilateration. Figure 11 shows the main elements of the acoustic positioning system.

An Attitude Heading Reference System board is installed inside each DOM. It is a chip that has an accelero-magnetic sensor that provides the three components of the Earth magnetic field and of the acceleration. From these components, the orientation of the DOM can be determined.

The position and orientation of the DOMs are the input data to the mechanical model used to reconstruct the shape of the DU by means of a simple mechanical model. Since the motion is small, we can assume, as a first approximation, that the anchored DU is in equilibrium between the buoyancy forces and the drag forces due to the sea current velocity, which is usually smaller than 10 cm/s. This produces a slight inclination of the line from the vertical, resulting usually in a displacement of a few meters in the upper DOMs in ORCA and tens of meters in those of ARCA. The weight/buoyancy and drag coefficient of the different elements are taken into account and the shape is determined by fitting the input data to the model using the sea current velocity as free parameter [143].
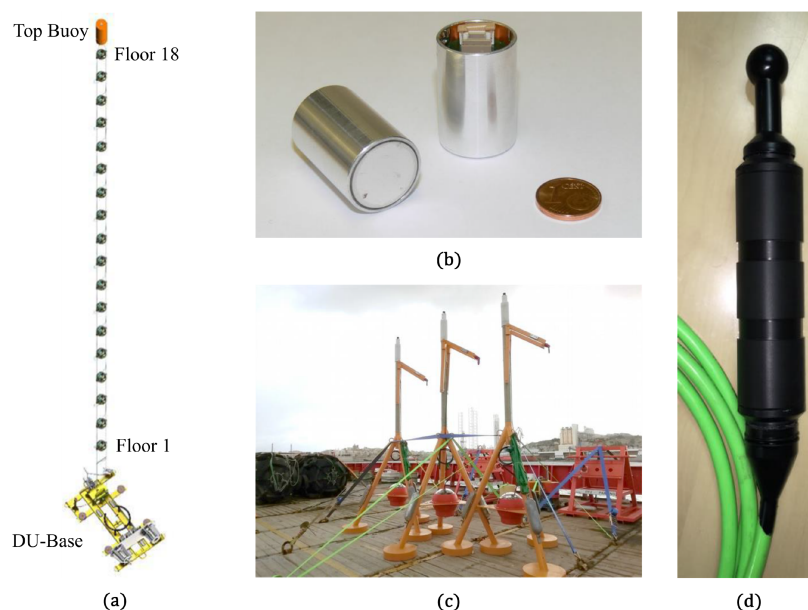
Figure 11. (**a**) Drawing of a KM3NeT DU, composed of an anchored base containing a hydrophone and 18 DOMs (labeled Floor 1, ..., Floor 18), and the top buoy; (**b**) Encapsulated piezoceramic acoustic sensor and electronic board with a pre-amplifier; (**c**) Three autonomous acoustic beacons before being deployed in ARCA; (**d**) Hydrophones used in KM3NeT (from Ref. [143]).

The KM3NeT Acoustic Beacon (AB) has been designed by the UPV group and developed in collaboration with Mediterráneo Señales Marítimas SLL company for being the emitter element of the Long Base Line positioning system of KM3NeT [17,18]. The AB is a broadband range acoustic emitter (20–60 kHz) able to work at rating depths up to 500 bars in an underwater environment. It provides the emission of short intense signals (sound pressure level larger than 180 dB re 1 µPa at 34 kHz). Each beacon can emit an arbitrary predefined signal. The AB is composed by a piezoceramic transducer and an electronic board integrated in an one-piece system by a cylindrical hard-anodised aluminium or titanium vessel, as it can be seen at the top element of the tripods in Figure 11c. The transducer is a commercial Free Flooded Ring SX30 manufactured by Sensor Technology Ltd., Collingwood, ON, Canada, The electronic board is specifically designed to fulfil the positioning system requirements, enabling the transducer communication and the signal emission control and amplification. It has a serial interface communication via RS232 for signal configuration from shore and a trigger line to emit the acoustic signal with a precision better than 1 µs. They can be operated in two modes: wired to the KM3NeT facility, i.e., synchronised and with all functionalities, or autonomous and fed with batteries, as the ones shown in Figure 11c.

6. Associated Sciences

The KM3NeT deep-sea detectors provide a unique facility for Earth-Sea Sciences studies for its capability to handle sophisticated monitoring sensor systems in real time in such environments. The contributions of the Spanish groups to the associated Earth-Sea Sciences on KM3NeT are mainly related to underwater noise assessment and bio-acoustic signal detection [144]. These activities are carried out through the collaboration framework defined by the 'Unidad Mixta de Investigación IEO-UPV en Tecnología para Estudios Marinos' (hereafter UTEM).

The study of the marine habitat has been promoted by the European member states through the Marine Strategy Framework Directive (MSFD) adopted in 2008 with the objective of protecting the sea environment in all European demarcations. The balance between human activities and the health of aquatic ecosystems is difficult, especially considering that anthropogenic pressures on the sea have increased over the last decades. The evalu-

ation of the potential adverse impact caused by human activities is being implemented through the development of 11 descriptors based on monitoring activities that help to achieve the Good Environmental Status (GES) related to them. The possibility to use the KM3NeT infrastructure to monitor the sea conditions enables to infer the state of the marine ecosystems and brings the opportunity to establish long term trends in relation to some marine attributes. Among the systems that constitute the detector, the APS presents a great potential in the study of the marine environment. The acoustic sensors placed in the bottom of the DUs can be used as a passive acoustic monitoring system. This links directly to the scope of descriptor 11 of the MSFD that is partially based on the in situ underwater acoustic noise measurements. Underwater acoustic passive monitoring represents a potential tool to study not only the presence of cetacean species by means of bio-acoustic based indicators, but also the influence of anthropogenic pressures on it.

The applications of real time KM3NeT underwater acoustic monitoring system are diverse: monitoring of underwater noise, the identification of marine species using algorithms for detecting bio-acoustic signals or through eco-acoustics [145] can be carried out perfectly in the KM3NeT marine science activity context. The viability of the underwater neutrino telescope used as an monitoring tool was demonstrated for example through the detection of long-range echolocation signals of sperm whales, reported by the ANTARES project [146].

The study of the underwater anthropogenic noise using KM3NeT is of great interest since it allows performing long term monitoring in almost real time because acoustic nodes are cabled to shore. The KM3NeT detectors can play a relevant role in the evaluation of continuous low frequency noise generated by marine traffic. The American Geophysical Union reports that marine traffic has increased almost a 300% over the last 20 years [147]. Among the initiatives carried out by different groups of experts (e.g., TGnoise) to develop methodologies to assess GES, the need to calculate threshold values stands out. The results that can be obtained through the KM3NeT detector are highly appreciated for filling the gap of measurements of the ambient level of noise in places where the influence of human activities is minimised. These types of studies are not easy to implement since sound is transmitted very efficiently in the water and it is difficult to find areas where the presence of boats is reduced. Considering the great depth of the KM3NeT installation ($\sim$2500 m for ORCA and 3500 m for ARCA), the noise measurements can help establish the baseline of continuous low frequency noise from which to calculate the excess level of noise due to marine traffic.

Data from March of 2020 to May of 2021 have been analysed and trends of underwater marine noise in 1/3 octave band of 63 Hz and 125 Hz are being extracted. Results will be very valuable from the point of view of the evaluation of environmental noise (following TGnoise guidelines). In addition, these results can serve to validate the simulations of noise in larger areas related to maritime traffic using Automatic Identification System (AIS) data.

Regarding the bioacoustic signal detection activities, it is mandatory to remark the importance of ORCA and ARCA location with respect to the marine mammal fauna. The ORCA site is located at the Algero Provençal basin near to the Pelagos Sanctuary for Mediterranean marine mammals [148]. This area represents an exceptional opportunity to study different aspects related to marine mammals due to the richness of cetacean inhabiting the zone. Studies regarding migration patterns, presence/absence of a given species or dial/seasonal use of habitat among many others aspects can be carried out by implementing automatic detection algorithms [144]. The performance of the bio-acoustic automatic detector was tested in terms of ambient noise level. The results show that a relationship of the efficiency of the whistle detector developed with respect to the noise present in the studied area exists. This is an important aspect to consider when developing presence models of cetacean species or tasks related to monitoring its vocalisation activity because noise can mask the presence of animals.

In summary, the KM3NeT infrastructure can play a relevant role in the field of marine sciences, especially in those areas related to underwater acoustics.

7. Summary and Outlook

Neutrino telescopes are exceptional tools with a very wide scientific scope. They were originally proposed as instruments to observe the Universe outside the Earth in a novel way thanks to the advantages of neutrinos as cosmic messengers—notwithstanding the challenges of their detection—but experience has shown that many other scientific goals are at their reach. These additional goals not only include topics related to fundamental physics—notably the study of neutrino properties and the search for new physics phenomena—but also other scientific areas, such as Sea Sciences, for which these facilities provide an exceedingly useful platform.

Several Spanish research teams have been involved during the last decades in the design, construction, operation and scientific exploitation of the ANTARES and KM3NeT neutrino telescopes. In this review, a selection of topics on which the Spanish contributions were most noticeable have been presented.

From the very beginning, the search for cosmic neutrino sources has been one of the priorities of these groups. The work done by the Spanish teams in neutrino astronomy include searches for diffuse and point-like neutrino sources and for correlations of neutrinos with transient astrophysical sources and related analyses in the context of multi-messenger astronomy.

The Spanish groups have led the search for possible accumulations of WIMP dark matter in the Sun or the Galactic Centre using neutrinos. ANTARES and KM3NeT are particularly well suited for dark matter searches in the direction of the Galactic Centre due to their geographical location. ANTARES limits for high-mass WIMPs in the Galactic Centre are particularly competitive, as shown in this article. The search for dark matter from the Sun has, as a by-product, set limits to a possible neutrino flux coming from standard CR interactions with the Sun. The recent commissioning of additional detector lines in ARCA and ORCA gives an extraordinary opportunity to improve the sensitivity of these searches in the near future.

The determination of the neutrino mass ordering has driven the design of the ORCA detector, but as shown in several analyses carried out by our groups, the potential of neutrino telescopes for other topics, like the search for neutrino non-standard interactions or neutrino decay, is large. Studies on the sensitivity of KM3NeT for NSIs and neutrino decay have already been performed, showing very promising results. The first analyses with real data with the present layout of the ORCA detector are progressing.

The Spanish contributions to ANTARES and KM3NeT include work on the time calibration and positioning systems, the electronics board design, production, testing and reliability, and the acoustic system, all of which have been briefly described.

Infrastructures like ANTARES and KM3NeT are also a great opportunity for sea science. An example is the study of the marine acoustic background, as shown in this article.

New DUs of KM3NeT have recently been installed, totalling up to 18 lines between both ARCA and ORCA, and the data taking is proceeding smoothly. The calibration of the new detector layout and the thorough understanding of its response are ongoing, while the first results of the analyses of the data taken by previous detector configurations are being obtained. Meanwhile, the deployment of new KM3NeT DUs is steadily progressing.

In the coming years, the KM3NeT detectors will be the flagship of the European neutrino astronomy community and will offer excellent scientific opportunities that the Spanish groups are willing to seize.

Author Contributions: J.J.H.-R., M.A., M.B.C., A.F.D., S.R.G., J.A.M.-M., S.N., D.R., D.C., F.S.G., A.S.L., J.d.D.Z. and J.Z. contributed equally to this article. All authors have read and agreed to the published version of the manuscript.

Abbreviations

The following abbreviations are used in this manuscript:

ANTARES	Astronomy with a Neutrino Telescope and Abyss Environmental RESearch
APS	Acoustic Positioning System
ARCA	Astronomy Research with Cosmics in the Abyss
BSM	Beyond Standard Model
CC	Charged Current
CLB	Central Logic Board
CR	Cosmic Ray
DM	Dark Matter
DOM	Digital Optical Module
EFT	Effective Field Theory
FPGA	Field Programmable Gate Arrays
GES	Good Environmental Status (GES)
GRB	Gamma-Ray Burst
GW	Gravitational Wave
LED	Light Emission Diode
LVDS	Low Voltage Differential Signal
MSFG	Marine Strategy Framework Directive
NC	Neutral Current
NSI	Non-Standard Interaction
ORCA	Oscillation Research with Cosmics in the Abyss
PB	Power Board
PMT	Photomultiplier Tube
PTP	Precision Time Protocol
SAν	Solar Atmospheric Neutrino
SFP	Small Form Factor Pluggable
SPI	Serial Peripheral Interface
TDC	Time-to-Digital Converter
TDE	Tidal Disruption Event
WIMP	Weakly Interacting Massive Particle

References

1. Aartsen, M.G. et al. [IceCube Collaboration] Evidence for High-Energy Extraterrestrial Neutrinos at the IceCube Detector. *Science* **2013**, *342*, 1242856. [CrossRef] [PubMed]
2. Aartsen, M.G. et al. [IceCube Collaboration] The IceCube Neutrino Observatory: Instrumentation and Online Systems. *JINST* **2017**, *12*, P03012. [CrossRef]
3. Markov, M.A.; Zheleznykh, I.M. On high energy neutrino physics in cosmic rays. *Nucl. Phys.* **1961**, *27*, 385–394. [CrossRef]
4. Ageron, M. et al. [ANTARES Collaboration] ANTARES: The first undersea neutrino telescope. *Nucl. Instrum. Meth. A* **2011**, *656*, 11–38. [CrossRef]
5. Adrian-Martinez, S.; Ageron, M.; Aharonian, F.; Aiello, S.; Albert, A.; Ameli, F.; Anassontzis, E.; Andre, M.; Androulakis, G.; Anghinolfi, M.; et al Letter of intent for KM3NeT 2.0. *J. Phys. G* **2016**, *43*, 084001. [CrossRef]
6. Aartsen, M.G.; Ageron, M.; Aharonian, F.; Aiello, S.; Albert, A.; Ameli, F.; Anassontzis, E.; Andre, M.; Androulakis, G.; Anghinolfi, M.; et al Observation of High-Energy Astrophysical Neutrinos in Three Years of IceCube Data. *Phys. Rev. Lett.* **2014**, *113*, 101101. [CrossRef] [PubMed]
7. Ackermann, M. et al. [The Fermi LAT collaboration] The spectrum of isotropic diffuse gamma-ray emission between 100 MeV and 820 GeV. *Astrophys. J.* **2015**, *799*, 86. [CrossRef]
8. Fenu, F. The cosmic ray energy spectrum measured using the Pierre Auger Observatory. *PoS* **2017**, *2017*, 9–16. [CrossRef]

9. Belolaptikov, I.; Dzhilkibaev, Z. Neutrino Telescope in Lake Baikal: Present and Nearest Future. *PoS* **2021**, *2021*, 2. [CrossRef]
10. Aguilar, J.A. et al. [The ANTARES Collaboration] Study of large hemispherical photomultiplier tubes for the antares neutrino telescope. *Nucl. Instrum. Meth. A* **2005**, *555*, 132–141. [CrossRef]
11. Ageron, M. et al. [ANTARES Collaboration] The ANTARES Optical Beacon System. *Nucl. Instrum. Meth. A* **2007**, *578*, 498–509. [CrossRef]
12. Aguilar, J.A. et al. [The ANTARES Collaboration] Time Calibration of the ANTARES Neutrino Telescope. *Astropart. Phys.* **2011**, *34*, 539–549. [CrossRef]
13. Adrián-Martínez, S.; Albert, A.; André, M.; Anton, G.; Ardid, M.; Aubert, J.-J.; Baret, B.; Barrios-Martí, J.; Basa, S.; Bertin, V.; et al. Time calibration with atmospheric muon tracks in the ANTARES neutrino telescope. *Astropart. Phys.* **2016**, *78*, 43–51. [CrossRef]
14. Emanuele, E.; Real, D.; Urbano, F.; de Dios Zornoza, J.; Zuniga, J. Development of a new laser beacon for time calibration in the ANTARES neutrino telescope. In Proceedings of the 8th IEEE International Conference on Mobile Ad-Hoc and Sensor Systems, MASS 2011, Valencia, Spain, 17–21 October 2011; Volume 6076706, pp. 904–909. [CrossRef]
15. Real, D.; Calvo, D. Nanobeacon and Laser Beacon: KM3NeT Time Calibration Devices. *PoS* **2015**, *2014*, 365. [CrossRef]
16. Real, D. Proposal of a new generation of Laser Beacon for time calibration in the KM3NeT neutrino telescope. *AIP Conf. Proc.* **2015**, *1630*, 130–133. [CrossRef]
17. Saldaña, M.; Adrián-Martínez, S.; Bou-Cabo, M.; Felis, I.; Larosa, G.; Llorens, C.D.; Martínez-Mora, J.A.; Ardid, M. Ultrasonic Transmitter for Positioning of the Large Underwater Neutrino Telescope KM3NeT. *Phys. Procedia* **2015**, *63*, 195–200. [CrossRef]
18. Ardid, M.; Martínez-Mora, J.A.; Bou-Cabo, M.; Larosa, G.; Adrián-Martínez, S.; Llorens, C.D. Acoustic Transmitters for Underwater Neutrino Telescopes. *Sensors* **2012**, *12*, 4113–4132. [CrossRef]
19. Ardid, M.; Bou-Cabo, M.; Camarena, F.; Espinosa, V.; Larosa, G.; Llorens, C.D.; Martinez-Mora, J.A. A prototype for the acoustic triangulation system of the KM3NeT deep sea neutrino telescope. *Nucl. Instrum. Meth. A* **2010**, *617*, 459–461. [CrossRef]
20. Saldaña, M.; Llorens, C.D.; Felis, I.; Martínez-Mora, J.A.; Ardid, M. Transducer Development and Characterization for Underwater Acoustic Neutrino Detection Calibration. *Sensors* **2016**, *16*, 1210. [CrossRef]
21. Calvo, D.; Real, D. Status of the central logic board (CLB) of the KM3NeT neutrino telescope. *JINST* **2015**, *10*, C12027. [CrossRef]
22. Real, D.; Calvo, D.; Musico, P.; Jansweijer, P.; van Beveren, V.; Colonges, S.; Pellegrini, G.; Díaz, A.F. KM3NeT Acquisition Electronics: New Developments and Advances in Reliability. *PoS* **2021**, *2021*, 1108. [CrossRef]
23. Real, D.; Bozza, C.; Calvo, D.; Musico, P.; Jansweijer, P.; Colonges, S.; van Beveren, V.; Versari, F.; Chiarusi, T.; Carriò, F.; et al. KM3NeT acquisition: The new version of the Central Logic Board and its related Power Board, with highlights and evolution of the Control Unit. *JINST* **2020**, *15*, C03024. [CrossRef]
24. Calvo, D.; Real, D.; Carrió, F. Sub-nanosecond synchronization node for high-energy astrophysics: The KM3NeT White Rabbit Node. *Nucl. Instrum. Meth. A* **2020**, *958*, 162777. [CrossRef]
25. Llorens, C.D.; Ardid, M.; Sogorb, T.; Bou-Cabo, M.; Martinez-Mora, J.A.; Larosa, G.; Adrian-Martinez, S. The Sound Emission Board of the KM3NeT Acoustic Positioning System. *JINST* **2012**, *7*, C01001. [CrossRef]
26. Real, D.; Calvo, D.; Illuminati, G.; Colonges, S. Reliability studies for KM3NeT electronics: The FIDES method. In Proceedings of the 35th International Cosmic Ray Conference, Busan, Korea, 10–20 July 2018; Volume 2017, p. 1003. [CrossRef]
27. Real, D.; Calvo, D.; Musico, P.; Jansweijer, P.; Colonges, S.; van Beveren, V.; Carriò, F.; Pellegrini, G.; Díaz, A.F. Reliability studies for the White Rabbit Switch in KM3NeT: FIDES and Highly Accelerated Life Tests. *JINST* **2020**, *15*, C02042. [CrossRef]
28. Illuminati, G. Searches for point-like sources of cosmic neutrinos with 13 years of ANTARES data. *PoS* **2021**, *2021*, 1161.
29. Aublin, J.; Illuminati, G.; Navas, S. Searches for point-like sources of cosmic neutrinos with 11 years of ANTARES data. *PoS* **2020**, *2019*, 920. [CrossRef]
30. Salesa-Greus, F. Search for point-like sources with the ANTARES neutrino telescope. In Proceedings of the 2nd Roma International Conference on Astroparticle Physics (RICAP 2009), Rome, Italy, 13–15 May 2011; Volume 630, pp. 214–217. [CrossRef]
31. Adrian-Martinez, S. et al. [ANTARES Collaboration] Search for Cosmic Neutrino Point Sources with Four Year Data of the ANTARES Telescope. *Astrophys. J.* **2012**, *760*, 53. [CrossRef]
32. Adrián-Martínez, S.; Albert, A.; André, M.; Anton, G.; Ardid, M.; Aubert, J.-J.; Baret, B.; Barrios-Martì, J.; Basa, S.; Bertin, V.; et al. Constraining the neutrino emission of gravitationally lensed Flat-Spectrum Radio Quasars with ANTARES data. *JCAP* **2014**, *11*, 17. [CrossRef]
33. Adrian-Martinez, S. et al. [ANTARES Collaboration] Searches for Point-like and extended neutrino sources close to the Galactic Centre using the ANTARES neutrino Telescope. *Astrophys. J. Lett.* **2014**, *786*, L5. [CrossRef]
34. Albert, A. et al. [ANTARES Collaboration] First all-flavor neutrino pointlike source search with the ANTARES neutrino telescope. *Phys. Rev. D* **2017**, *96*, 082001. [CrossRef]
35. Adrian-Martinez, S. et al. [ANTARES Collaboration] The First Combined Search for Neutrino Point-sources in the Southern Hemisphere With the Antares and Icecube Neutrino Telescopes. *Astrophys. J.* **2016**, *823*, 65. [CrossRef]
36. Albert, A. et al. [ANTARES Collaboration] ANTARES and IceCube Combined Search for Neutrino Point-like and Extended Sources in the Southern Sky. *Astrophys. J.* **2020**, *892*, 92. [CrossRef]
37. Albert, A. et al. [ANTARES Collaboration] All-flavor Search for a Diffuse Flux of Cosmic Neutrinos with Nine Years of ANTARES Data. *Astrophys. J. Lett.* **2018**, *853*, L7. [CrossRef]
38. Eberl, T.; Navas, S.; Versari, F.; Fusco, L.A. Search for a diffuse flux of cosmic neutrinos with the ANTARES telescope. *PoS* **2018**, *2017*, 993. [CrossRef]

39. Adrian-Martinez, S.; Al Samarai, I.; Albert, A.; André, M.; Anghinolfi, M.; Anton, G.; Anvar, S.; Ardid, M.; Astraatmadja, T.; Aubert, J.-J.; et al. Search for Neutrino Emission from Gamma-Ray Flaring Blazars with the ANTARES Telescope. *Astropart. Phys.* **2012**, *36*, 204–210. [CrossRef]

40. Adrian-Martinez, S.; Albert, A.; André, M.; Anton, G.; Ardid, M.; Aubert, J.-J.; Baret, B.; Barrios-Martí, J.; Basa, S.; Bertin, V.; et al. Search for muon-neutrino emission from GeV and TeV gamma-ray flaring blazars using five years of data of the ANTARES telescope. *JCAP* **2015**, *12*, 14. [CrossRef]

41. Albert, A.; André, M.; Anton, G.; Ardid, M.; Aubert, J.-J.; Avgitas, T.; Baret, B.; Barrios-Martí, J.; Basa, S.; Bertin, V.; et al. Time-dependent search for neutrino emission from x-ray binaries with the ANTARES telescope. *JCAP* **2017**, *4*, 19. [CrossRef]

42. Albert, A. et al. [ANTARES Collaboration] ANTARES neutrino search for time and space correlations with IceCube high-energy neutrino events. *Astrophys. J.* **2019**, *879*, 108. [CrossRef]

43. Albert, A.; Andrè, M.; Anghinolfi, M.; Anton, G.; Ardid, M.; Aubert, J.-J.; Aublin, J.; Avgitas, T.; Baret, B.; Barrios-Martì, J.; et al. The Search for Neutrinos from TXS 0506+056 with the ANTARES Telescope. *Astrophys. J. Lett.* **2018**, *863*, L30. [CrossRef]

44. Palacios González, J. KM3NeT/ARCA sensitivity to transient neutrino sources. *PoS* **2021**, *2021*, 1162.

45. Alves Garre, S. ANTARES offline study of three alerts after Baikal-GVD follow-up found coincident cascade neutrino events. *PoS* **2021**, *2021*, 1121.

46. Adrian-Martinez, S. et al. [ANTARES Collaboration] First results on dark matter annihilation in the Sun using the ANTARES neutrino telescope. *JCAP* **2013**, *11*, 32. [CrossRef]

47. Adrián-Martínez, S.; Albert, A.; André, M.; Anton, G.; Ardid, M.; Aubert, J.-J.; Avgitas, T.; Baret, B.; Barrios-Martí, J.; Basa, S.; et al. A search for Secluded Dark Matter in the Sun with the ANTARES neutrino telescope. *JCAP* **2016**, *5*, 16. [CrossRef]

48. Adrian-Martinez, S. et al. [ANTARES Collaboration] Limits on Dark Matter Annihilation in the Sun using the ANTARES Neutrino Telescope. *Phys. Lett. B* **2016**, *759*, 69–74. [CrossRef]

49. Lopez-Coto, D.; Navas, S.; Zornoza, J.D. Dark Matter Searches from the Sun with the KM3NeT-ORCA detector. *PoS* **2020**, *2019*, 536. [CrossRef]

50. Hernandez-Rey, J.J.; Lambard, G. Indirect search for dark matter with the ANTARES neutrino telescope. In Proceedings of the 33rd International Cosmic Ray Conference, Rio de Janeiro, Brazil, 2–9 July 2013; p. 0613.

51. Adrian-Martinez, S. et al. [ANTARES Collaboration] Search of Dark Matter Annihilation in the Galactic Centre using the ANTARES Neutrino Telescope. *JCAP* **2015**, *10*, 68. [CrossRef]

52. Albert, A.; André, M.; Anghinolfi, M.; Anton, G.; Ardid, M.; Aubert, J.J.; Aublin, J.; Baret, B.; Basa, S.; Belhorma, B.; et al. Search for dark matter towards the Galactic Centre with 11 years of ANTARES data. *Phys. Lett. B* **2020**, *805*, 135439. [CrossRef]

53. Albert, A.; André, M.; Anghinolfi, M.; Ardid, M.; Aubert, J.J.; Aublin, J.; Baret, B.; Basa, S.; Belhorma, B.; Bertin, V.; et al. Combined search for neutrinos from dark matter self-annihilation in the Galactic Center with ANTARES and IceCube. *Phys. Rev. D* **2020**, *102*, 082002. [CrossRef]

54. Gozzini, S.R.; Iovine, N.; Sánchez, J.A.A.; Baur, S.; de Dios Zornoza Gómez, J. Combined search for dark matter from the Galactic Centre with the ANTARES and IceCube neutrino telescopes. *EPJ Web Conf.* **2019**, *207*, 04007. [CrossRef]

55. Gozzini, S.; Sala, F.; Zornoza, J.D. Search for heavy secluded dark matter with ANTARES. In Proceedings of the Neutrino 2020, Chicago, IL, USA, 21–27 June 2020.

56. Manczak, J.; Chowdhury, N.R.K.; Hernández-Rey, J.J. Neutrino non-standard interactions with the KM3NeT/ORCA detector. *PoS* **2021**, *2021*, 1165. [CrossRef]

57. Hernández Rey, J.J.; Khan Chowdhury, N.R.; Manczak, J.; Navas, S.; Zornoza, J.D. Search for neutrino non-standard interactions with ANTARES and KM3NeT-ORCA. *JINST* **2021**, *16*, C09016. [CrossRef]

58. Khan Chowdhury, N.R. Neutrino Oscillations and Non-standard Interactions with KM3NeT-ORCA. In Proceedings of the Prospects in Neutrino Physics, London, UK, 16–18 December 2020.

59. de Salas, P.F.; Pastor, S.; Ternes, C.A.; Thakore, T.; Tórtola, M. Constraining the invisible neutrino decay with KM3NeT-ORCA. *Phys. Lett. B* **2019**, *789*, 472–479. [CrossRef]

60. Zyla, P.A.; Amsler, C.D.; Asner, D.M.; Bamett, R.M.; Beringer, J.; Burchat, P.R.; Carone, C.D.; Caso, C.; Dahl, O.I.; D'Ambrosio, G.; et al. Review of Particle Physics. *PTEP* **2020**, *2020*, 083C01. [CrossRef]

61. Engel, R. Highlights from the Pierre Auger Observatory. *PoS* **2021**, *2021*, 021.

62. Klebesadel, R.W.; Strong, I.B.; Olson, R.A. Observations of Gamma-Ray Bursts of Cosmic Origin. *Astrophys. J. Lett.* **1973**, *182*, L85–L88. [CrossRef]

63. Wakely, S.P.; Horan, D. TeVCat: An online catalog for Very High Energy Gamma-Ray Astronomy. In Proceedings of the 30th International Cosmic Ray Conference, Merida, Mexico, 3–11 July 2007; Volume 3, pp. 1341–1344.

64. Abbott, B.P. et al. [The LIGO Scientific Collaboration] Observation of Gravitational Waves from a Binary Black Hole Merger. *Phys. Rev. Lett.* **2016**, *116*, 061102. [CrossRef]

65. Abbott, R.; Abbott, T.D.; Acernese, F.; Ackley, K.; Adams, C.; Adhikari, N.; Adhikari, R.X.; Adya, V.B.; Affeldt, C.; Agarwal, D.; et al. GWTC-3: Compact Binary Coalescences Observed by LIGO and Virgo During the Second Part of the Third Observing Run. *arXiv* **2021**, arXiv:2111.03606.

66. Akutsu, T.; Ando, M.; Arai, K.; Arai, Y.; Araki, S.; Araya, A.; Aritomi, N.; Asada, H.; Aso, Y.; Atsuta, S.; et al. KAGRA: 2.5 Generation Interferometric Gravitational Wave Detector. *Nature Astron.* **2019**, *3*, 35–40. [CrossRef]

67. Greus, F.S.; Losa, A.S. Multimessenger Astronomy with Neutrinos. *Universe* **2021**, *7*, 397. [CrossRef]

68. Fusco, L.A. Search for a diffuse flux of cosmic neutrinos with the ANTARES neutrino telescope. *PoS* **2021**, *2021*, 1126. [CrossRef]

69. Aartsen, M.G. et al. [IceCube Collaboration] Time-Integrated Neutrino Source Searches with 10 Years of IceCube Data. *Phys. Rev. Lett.* **2020**, *124*, 051103. [CrossRef] [PubMed]

70. Muller, R.; Heijboer, A.; Soto, A.G.; Caiffi, B.; Sanguineti, M.; Kulikovskiy, V. Sensitivity estimates for diffuse, point-like and extended neutrino sources with KM3NeT/ARCA. *PoS* **2021**, *2021*, 1077.

71. Aartsen, M.G. et al. [The IceCube] Multimessenger observations of a flaring blazar coincident with high-energy neutrino IceCube-170922A. *Science* **2018**, *361*, eaat1378. [CrossRef] [PubMed]

72. Aartsen, M.G. et al. [IceCube Collaboration] Neutrino emission from the direction of the blazar TXS 0506+056 prior to the IceCube-170922A alert. *Science* **2018**, *361*, 147–151. [CrossRef] [PubMed]

73. Oikonomou, F. High-energy neutrino emission from blazars. *PoS* **2021**, *2021*, 30.

74. Plavin, A.V.; Kovalev, Y.Y.; Kovalev, Y.A.; Troitsky, S.V. Directional Association of TeV to PeV Astrophysical Neutrinos with Radio Blazars. *Astrophys. J.* **2021**, *908*, 157. [CrossRef]

75. Plavin, A.; Kovalev, Y.Y.; Kovalev, Y.A.; Troitsky, S. Observational Evidence for the Origin of High-energy Neutrinos in Parsec-scale Nuclei of Radio-bright Active Galaxies. *Astrophys. J.* **2020**, *894*, 101. [CrossRef]

76. Albert, A.; André, M.; Anghinolfi, M.; Anton, G.; Ardid, M.; Aubert, J.-J.; Aublin, J.; Baret, B.; Basa, S.; Belhorma, B.; et al. ANTARES Search for Point Sources of Neutrinos Using Astrophysical Catalogs: A Likelihood Analysis. *Astrophys. J.* **2021**, *911*, 48. [CrossRef]

77. Illuminati, G. ANTARES search for neutrino flares from the direction of radio-bright blazars. *PoS* **2021**, *2021*, 972.

78. Stein, R.; van Velzen, S.; Kowalski, M.; Franckowiak, A.; Gezari, S.; Miller-Jones, J.C.A.; Frederick, S.; Sfaradi, I.; Bietenholz, M.F.; Horesh, A.; et al. A tidal disruption event coincident with a high-energy neutrino. *Nature Astron.* **2021**, *5*, 510–518. [CrossRef]

79. Wang, X.Y.; Liu, R.Y.; Dai, Z.G.; Cheng, K.S. Probing the tidal disruption flares of massive black holes with high-energy neutrinos. *Phys. Rev. D* **2011**, *84*, 081301. [CrossRef]

80. Stein, R. Tidal Disruption Events and High-Energy Neutrinos. *PoS* **2021**, *2021*, 9.

81. Albert, A. et al. [ANTARES Collaboration] Search for neutrinos from the tidal disruption events AT2019dsg and AT2019fdr with the ANTARES telescope. *Astrophys. J.* **2021**, *920*, 50. [CrossRef]

82. Waxman, E.; Bahcall, J.N. High-energy neutrinos from cosmological gamma-ray burst fireballs. *Phys. Rev. Lett.* **1997**, *78*, 2292–2295. [CrossRef]

83. Kimura, S.S.; Murase, K.; Bartos, I.; Ioka, K.; Heng, I.S.; Mészáros, P. Transejecta high-energy neutrino emission from binary neutron star mergers. *Phys. Rev. D* **2018**, *98*, 043020. [CrossRef]

84. Abbott, B.P. et al. [LIGO Scientific Collaboration] Multi-messenger Observations of a Binary Neutron Star Merger. *Astrophys. J. Lett.* **2017**, *848*, L12. [CrossRef]

85. Coleiro, A.; Colomer Molla, M.; Dornic, D.; Lincetto, M.; Kulikovskiy, V. Combining neutrino experimental light-curves for pointing to the next galactic core-collapse supernova. *Eur. Phys. J. C* **2020**, *80*, 856. [CrossRef]

86. Aiello, S. et al. [KM3NeT Collaboration] The KM3NeT potential for the next core-collapse supernova observation with neutrinos. *Eur. Phys. J. C* **2021**, *81*, 445. [CrossRef]

87. Albert, A.; Andre, M.; Anghinolfi, M.; Ardid, M.; Aubert, J.-J.; Aublin, J.; Avgitas, T.; Baret, B.; Barrios-Marti, J.; Basa, S.; et al. Search for High-energy Neutrinos from Binary Neutron Star Merger GW170817 with ANTARES, IceCube, and the Pierre Auger Observatory. *Astrophys. J. Lett.* **2017**, *850*, L35. [CrossRef]

88. Avrorin, A.D. et al. [Baikal-GVD Collaboration] Search for High-Energy Neutrinos from GW170817 with the Baikal-GVD Neutrino Telescope. *JETP Lett.* **2018**, *108*, 787–790. [CrossRef]

89. Albert, A. et al. [ANTARES Collaboration] All-sky search for high-energy neutrinos from gravitational wave event GW170104 with the Antares neutrino telescope. *Eur. Phys. J. C* **2017**, *77*, 911. [CrossRef]

90. Albert, A. et al. [ANTARES Collaboration] Search for neutrino counterparts of gravitational-wave events detected by LIGO and Virgo during run O$_2$ with the ANTARES telescope. *Eur. Phys. J. C* **2020**, *80*, 487. [CrossRef]

91. Albert, A. et al. [ANTARES Collaboration] ANTARES upper limits on the multi-TeV neutrino emission from the GRBs detected by IACTs. *JCAP* **2021**, *3*, 92. [CrossRef]

92. Cao, Z.; Aharonian, F.; An, Q.; Axikegu; Bai, L.X.; Bai, Y.X.; Bao, Y.W.; Bastieri, D.; Bi, X.J.; Bi, Y.J.; et al. Ultrahigh-energy photons up to 1.4 petaelectronvolts from 12 γ-ray Galactic sources. *Nature* **2021**, *594*, 33–36. [CrossRef] [PubMed]

93. Amenomori, M.; Bao, Y.W.; Bi, X.J.; Chen, D.; Chen, T.L.; Chen, W.Y.; Chen, X.; Chen, Y.; Cirennima; Cui, S.W.; et al. First Detection of sub-PeV Diffuse Gamma Rays from the Galactic Disk: Evidence for Ubiquitous Galactic Cosmic Rays beyond PeV Energies. *Phys. Rev. Lett.* **2021**, *126*, 141101. [CrossRef] [PubMed]

94. Adrian-Martinez, S.; Albert, A.; André, M.; Anghinolfi, M.; Anton, G.; Ardid, M.; Aubert, J.-J.; Avgitas, T.; Baret, B.; Barrios-Martí, J.; et al. Constraints on the neutrino emission from the Galactic Ridge with the ANTARES telescope. *Phys. Lett. B* **2016**, *760*, 143–148. [CrossRef]

95. Ferrara, G.; Fusco, L. Search for correlations between high-energy gamma rays and neutrinos with the HAWC and ANTARES detectors. *PoS* **2021**, *2021*, 962.

96. Niro, V.; Neronov, A.; Fusco, L.; Gabici, S.; Semikoz, D. Neutrinos from the gamma-ray source eHWC J1825-134: Predictions for Km3 detectors. *Phys. Rev. D* **2021**, *104*, 023017. [CrossRef]

97. Zornoza, J.D.D. Review on Indirect Dark Matter Searches with Neutrino Telescopes. *Universe* **2021**, *7*, 415. [CrossRef]

98. Aartsen, M.G. et al. [IceCube Collaboration] Search for Neutrinos from Dark Matter Self-Annihilations in the center of the Milky Way with 3 years of IceCube/DeepCore. *Eur. Phys. J. C* **2017**, *77*, 627. [CrossRef]

99. Abdallah, H. et al. [H.E.S.S. Collaboration] Search for dark matter annihilations towards the inner Galactic halo from 10 years of observations with H.E.S.S. *Phys. Rev. Lett.* **2016**, *117*, 111301. [CrossRef] [PubMed]

100. Archambault, S. et al. [VERITAS Collaboration] Dark Matter Constraints from a Joint Analysis of Dwarf Spheroidal Galaxy Observations with VERITAS. *Phys. Rev. D* **2017**, *95*, 082001. [CrossRef]

101. Ahnen, M.L.; Ansoldi, S.; Antonelli, L.A.; Antoranz, P.; Babic, A.; Banerjee, B.; Bangale, P.; Barres de Almeida, U.; Barrio, J.A.; Becerra González, J.; et al. Limits to Dark Matter Annihilation Cross-Section from a Combined Analysis of MAGIC and Fermi-LAT Observations of Dwarf Satellite Galaxies. *JCAP* **2016**, *2*, 39. [CrossRef]

102. Navarro, J.F.; Frenk, C.S.; White, S.D.M. The Structure of cold dark matter halos. *Astrophys. J.* **1996**, *462*, 563–575. [CrossRef]

103. Pospelov, M.; Ritz, A.; Voloshin, M.B. Secluded WIMP Dark Matter. *Phys. Lett. B* **2008**, *662*, 53–61. [CrossRef]

104. Ardid, M.; Felis, I.; Herrero, A.; Martínez-Mora, J.A. Constraining Secluded Dark Matter models with the public data from the 79-string IceCube search for dark matter in the Sun. *JCAP* **2017**, *4*, 10. [CrossRef]

105. Frankiewicz, K. Searching for Dark Matter Annihilation into Neutrinos with Super-Kamiokande. *arXiv* **2015**, arXiv:1510.07999.

106. Amole, C.; Ardid, M.; Arnquist, I.J.; Asner, D.M.; Baxter, D.; Behnke, E.; Bhattacharjee, P.; Borsodi, H.; Bou-Cabo, M.; Campion, P.; et al. Dark Matter Search Results from the PICO-60 C_3F_8 Bubble Chamber. *Phys. Rev. Lett.* **2017**, *118*, 251301. [CrossRef]

107. Moskalenko, I.V.; Karakula, S. Very high-energy neutrinos from the sun. *J. Phys. G* **1993**, *19*, 1399–1406. [CrossRef]

108. Ardid., M.; Felis, I.; Lotze, M.; Tönnis, C. Neutrinos from Cosmic Ray Interactions in the Sun as background for dark matter searches. *PoS* **2018**, *2017*, 907. [CrossRef]

109. Lopez-Coto, D.; Navas, S.; Zornoza, J.D. Solar Atmospheric Neutrinos searches with ANTARES neutrino telescope. *PoS* **2021**, *2021*, 1122. [CrossRef]

110. Gaisser, T.K. Spectrum of cosmic-ray nucleons, kaon production, and the atmospheric muon charge ratio. *Astropart. Phys.* **2012**, *35*, 801–806. [CrossRef]

111. Gaisser, T.K.; Stanev, T.; Tilav, S. Cosmic Ray Energy Spectrum from Measurements of Air Showers. *Front. Phys.* **2013**, *8*, 748–758. [CrossRef]

112. Serenelli, A.M.; Basu, S.; Ferguson, J.W.; Asplund, M. New solar composition: The problem with solar models revisited. *Astrophys. J. Lett.* **2009**, *705*, L123–L127. [CrossRef]

113. Grevesse, N.; Sauval, A.J. Standard Solar Composition. *Space Sci. Rev.* **1998**, *85*, 161–174. [CrossRef]

114. Bischer, I.; Rodejohann, W. General neutrino interactions from an effective field theory perspective. *Nucl. Phys. B* **2019**, *947*, 114746. [CrossRef]

115. Ohlsson, T. Status of non-standard neutrino interactions. *Rept. Prog. Phys.* **2013**, *76*, 044201. [CrossRef]

116. Miranda, O.G.; Nunokawa, H. Non standard neutrino interactions: Current status and future prospects. *New J. Phys.* **2015**, *17*, 095002. [CrossRef]

117. Fornengo, N.; Maltoni, M.; Tomas, R.; Valle, J.W.F. Probing neutrino nonstandard interactions with atmospheric neutrino data. *Phys. Rev. D* **2002**, *65*, 013010. [CrossRef]

118. Gonzalez-Garcia, M.C.; Maltoni, M. Atmospheric neutrino oscillations and new physics. *Phys. Rev. D* **2004**, *70*, 033010. [CrossRef]

119. Farzan, Y.; Tortola, M. Neutrino oscillations and Non-Standard Interactions. *Front. Phys.* **2018**, *6*, 10. [CrossRef]

120. Dev, P.S.; Babu, K.S.; Denton, P.B.; Machado, P.A.; Argüelles, C.A.; Barrow, J.L.; Chatterjee, S.S.; Chen, M.C.; de Gouvêa, A.; Dutta, B.; et al. Neutrino Non-Standard Interactions: A Status Report. *Sci. Post Phys. Proc.* **2019**, *2019*, 1. [CrossRef]

121. Esteban, I.; Gonzalez-Garcia, M.C.; Maltoni, M.; Martinez-Soler, I.; Salvado, J. Updated constraints on non-standard interactions from global analysis of oscillation data. *JHEP* **2018**, *8*, 180. [CrossRef]

122. Albert, A. et al. [ANTARES Collaboration] Measuring the atmospheric neutrino oscillation parameters and constraining the 3+1 neutrino model with ten years of ANTARES data. *JHEP* **2019**, *6*, 113. [CrossRef]

123. Mitsuka, G.; Abe, K.; Hayato, Y.; Iida, T.; Ikeda, M.; Kameda, J.; Koshio, Y.; Miura, M.; Moriyama, S.; Nakahata, M.; et al. Study of Non-Standard Neutrino Interactions with Atmospheric Neutrino Data in Super-Kamiokande I and II. *Phys. Rev.* **2011**, *D84*, 113008. [CrossRef]

124. Aartsen, M.G. et al. [IceCube Collaboration] Search for Nonstandard Neutrino Interactions with IceCube DeepCore. *Phys. Rev.* **2018**, *D97*, 072009. [CrossRef]

125. Schechter, J.V.J. Neutrino decay and spontaneous violation of lepton number. *Phys. Rev. D* **1982**, *25*, 774. doi:10.1103/PhysRevD.25.774. [CrossRef]

126. Acker, A.; Pantaleone, S.P.J. Decaying Dirac neutrinos. *Phys. Rev. D* **1992**, *45*, 1. [CrossRef]

127. Kapustinsky, J.; DeVries, R.; DiGiacomo, N.; Sondheim, W.; Sunier, J.; Coombes, H. A fast timing light pulser for scintillation detectors. In *Nuclear Instruments and Methods in Physics Research Section A: Accelerators, Spectrometers, Detectors and Associated Equipment*; Elsevier: Amsterdam, The Netherlands, 1985; Volume 241, pp. 612–613. [CrossRef]

128. Ricobenne, G. NEMO: NEutrino Mediterranean Observatory. In *Astrophysical Sources of High Energy Particles and Radiation*; Springer: Berlin, Germany, 2001; Volume 44, pp. 355–361. [CrossRef]

129. Martinez-S, A.; Aiello, S.; Ameli, F.; Anghinolfi, M.; Ardid, M.; Barbarino, G.; Barbarito, E.; Barbato, F.C.T.; Beverini, N.; Biagi, S.; et al. Long term monitoring of the optical background in the Capo Passero deep-sea site with the NEMO tower prototype. *Eur. Phys. J. C* **2016**, *76*, 1–11. [CrossRef]

130. Aiello, S.; Albert, A.; Alshamsi, M.; Garre, S.A.; Aly, Z.; Ambrosone, A.; Ameli, F.; Andre, M.; Androulakis, G.; Anghinolfi, M.; et al. Nanobeacon: A time calibration device for the KM3NeT neutrino telescope. *arXiv* **2021**, arXiv:2111.00223.

131. Real, D. The electronics readout and data acquisition system of the KM3NeT neutrino telescope node. *AIP Conf. Proc.* **2015**, *1630*, 102–105. [CrossRef]

132. Aiello, S. et al. [The KM3NeT Collaboration] KM3NeT front-end and readout electronics system: Hardware, firmware and software. *J. Astron. Telesc. Instrum. Syst.* **2019**, *5*, 046001. [CrossRef]

133. Real, D.; Calvo, D. Digital optical module electronics of KM3NeT. *Phys. Part. Nucl.* **2016**, *47*, 918–925. [CrossRef]

134. Aiello, S.; Albert, A.; Garre, S.A.; Aly, Z.; Ameli, F.; Andre, M.; Androulakis, G.; Anghinolfi, M.; Anguita, M.; Anton, G.; et al. Architecture and performance of the KM3NeT front-end firmware. *J. Astron. Telesc. Instrum. Syst.* **2021**, *7*, 016001. [CrossRef]

135. Real, D.; Calvo, D.; van Beveren, V.; Musico, P.; Pellegini, G.; Jansweijer, P.; Colonges, S.; Chiarusi, T.; Bozza, C.; Nicolau, C.; et al. Status of the DOM electronics. *JINST* **2021**, *16*, C10009. [CrossRef]

136. Real, D.; Calvo, D.; Musico, P.; Jansweijer, P.; Van Elewyck, V. KM3NeT Front-end electronics upgrade: CLBv3 and PBv3. *PoS* **2018**, *2017*, 1004. [CrossRef]

137. Lipinski, M.; Wlostowski, T.; Alvarez, P.J.S. White Rabbit: A PTP Application for Robust Sub-nanosecond Synchronization. In Proceedings of the IEEE International Symposium on Precision Clock Synchronization for Measurement, Control and Communication, Munich, Germany, 14–16 September 2011; pp. 25–30. [CrossRef]

138. Colonges, S.; Real, D.; Calvo, D.; Musico, P.; Pellegini, G.; Jansweijer, P.; van Beveren, V.; Chiarusi, T.; Bozza, C.; Nicolau, C.; et al. Electronics reliability methods for neutrinos telescopes: The KM3NeT case. *JINST* **2021**, *16*, C10010. [CrossRef]

139. Ardid, M. Positioning system of the ANTARES neutrino telescope. *Nucl. Instrum. Meth. A* **2009**, *602*, 174–176. [CrossRef]

140. Adrian-Martinez, S.; Ageron, M.; Aguilar, J.A.; Al Samarai, I.; Albert, A.; André, M.; Anghinolfi, M.; Anton, G.; Anvar, S.; Ardid, M.; et al. The Positioning System of the ANTARES Neutrino Telescope. *JINST* **2012**, *7*, T08002. [CrossRef]

141. Viola, S.; Ardid, M.; Bertin, V.; Enzenhöfer, A.; Keller, P.; Lahmann, R.; Larosa, G.; Llorens, C.D. NEMO-SMO acoustic array: A deep-sea test of a novel acoustic positioning system for a km^3-scale underwater neutrino telescope. *Nucl. Instrum. Meth. A* **2013**, *725*, 207–210. [CrossRef]

142. Poirè, C. et al. [KM3NeT Collaboration] KM3NeT Detection Unit Line Fit reconstruction using positioning sensors data. *PoS* **2021**, *2021*, 1052. [CrossRef]

143. Tortosa, D.D. Monitoring and Reconstruction of the Shape of the Detection Units in KM3NeT Using Acoustic and Compass Sensors. *Sensors* **2020**, *20*, 5116. [CrossRef] [PubMed]

144. Guidi, C.; Bou-Cabo, M.; Lara, G. Passive acoustic monitoring of cetaceans with KM3NeT acoustic receivers. *J. Instrum.* **2021**, *16*, C10004. [CrossRef]

145. Farina, A.; Gage, S.H. *Ecoacoustics: The Ecological Role of Sounds*, 1st ed.; John Wiley & Sons: Hoboken, NJ, USA, 2017.

146. Andre, M.; Caballé, A.; Van der Schaar, M.; Solsona, A.; Houégnigan, L.; Zaugg, S.; Sánchez, A.M.; Castell, J.V.; Solé, M.; Vila, F.; et al. Sperm whale long-range echolocation sounds revealed by ANTARES, a deep-sea neutrino telescope. *Sci. Rep.* **2017**, *7*, 45517. [CrossRef] [PubMed]

147. Tournadre, J. Anthropogenic pressure on the open ocean: The growth of ship traffic revealed by altimeter data analysis. *Geophys. Res. Lett.* **2014**, *41*, 7924–7932. [CrossRef]

148. Notarbartolo-di-Sciara, G.; Agardy, T.; Hyrenbach, D.; Scovazzi, T.; Van Klaveren, P. The Pelagos Sanctuary for Mediterranean marine mammals. *Conserv. Mar. Freshw. Ecosyst.* **2008**, *18*, 367–391. [CrossRef]